To the Graduate Council:

I am submitting herewith a thesis written by Ming Xu entitled "Adaptive Attenuation Correction Tool". I have examined the final copy of this thesis for form and content and recommend that it be accepted in partial fulfillment of the requirements for the degree of Master of Science, with a major in Electrical Engineering.

Dragana Brzakovic, Major Professor

We have read this thesis and recommend its acceptance:

Accepted for the Council:

Associate Vice Chancellor and Dean of the Graduate School

ADAPTIVE ATTENUATION CORRECTION TOOL

A Thesis
Presented for the
Master of Science
Degree
The University of Tennessee, Knoxville

Ming Xu

May 1992

ACKNOWLEDGEMENT

I would like to thank Dr. Gary T Smith, M.D., whose initiative made it possible for me to study and work in the area of nuclear medicine imaging, and taught me so much during his daily guidance. As major director of this project, Dr. Gary T Smith devoted a tremendous amount of time in directing my research. I am also very grateful to Dr. Dragana Brzakovic, for her time and enthusiasm in guiding the research and correcting the thesis drafts. Dr. Dragana Brzakovic instructed me in image processing techniques towards this research and provided the equipments and software. I would also like to thank the University of Tennessee Medical Center and its Radiology Department for the use of their equipment and financial support.

My gratitude also goes to Dr. George Kabalka, the other member of my committee, for his helping to made my research possible in the UT Medical Center. I would also like to thank Mr. Larry Byars, Mr. Paul Luk and other persons at Siemens/CTI PET System, Inc., for their liberal release of source codes and kind help in the completion of this research work.

I would like to take this opportunity to thank Mr. Shawn Steven for his technical help in writing thesis drafts. During the last year, Shawn has become a dear friend.

Finally, this thesis and research work would not have become a reality without the loving support of my wife, Hong Shen, whose undying encouragement and candid comments have given me much inspiration during the entire process. To my beloved wife, I owe many of my accomplishments in all aspects of my life.

ABSTRACT

The purpose of this research was to develop an effective method for attenuation correction for Positron Emission Tomography (PET). This involved the study of the principle of the attenuation problem, methodology of attenuation correction by using transmission scan images, image processing and segmentation of transmission images and software development for the graphic user interface used to fulfill the procedure.

Attenuation is the predominant quality problem of quantitative PET studies. Conventional attenuation correction methods use either predefined geometrical attenuation material shapes (calculated method), or directly use the transmission scan image for attenuation correction (measured method). Due to the simplicity of these methods, poor results are inevitable. Attenuation problem thus makes clinical PET diagnosis even more difficult.

The Adaptive Attenuation Correction Tool introduced here is a complete, user-friendly graphic user interface package. This tool provides an improved measured attenuation correction method by combining transmission image processing and interactive boundary redrawing options. The algorithm of image processing on the transmission scan was developed by modeling the low-count transmission and noise distribution. In addition to the image processing of the transmission scan images, the tool also provides interactive options and monitors intermediate results which gives the operators more control of attenuation correction throughout the whole process.

A comparison of this tool with the conventional methods reveals significant improvements. It requires much shorter transmission scanning time while producing better attenuation correction results. Clinical use of the technology should result in a dramatic reduction of patient bed-time and potentially better quantitative PET studies.

Key Words --- Positron Emission Tomography, attenuation correction, band-pass filtering, object oriented programming, graphic user interface

TABLE OF CONTENTS

CHAPTER 1.INTRODUCTION 1

1.1 Scope of Project 1

1.2 Statement of Problem 2

1.3 Rationale of the Project 5

1.4 Outline of the Thesis 6

CHAPTER 2.METHODOLOGY 8

2.1 Nature of Problem 8

2.1.1 Basic Principles of PET 8

2.1.2 Interaction Between Photons and Matter 9

2.1.3 Attenuation of the Annihilation Photons 11

2.1.4 Mathematical Correction of Attenuation 12

2.2 Corrections for Attenuation 13

2.2.1 Calculated Attenuation Correction 13

2.2.2 Measured Attenuation Correction 15

2.2.3 Combined Measured and Calculated Attenuation Correction 16

2.3 Review of Previous Works 16

2.4 The Adaptive Attenuation Correction Tool 18

CHAPTER 3.IMAGE SEGMENTATION 20

3.1 General Procedures 20

3.1.1 Dual Approaches 21

3.1.2 Multi-Step Segmentation Scheme 21

3.1.3 Interactive Procedures 22

3.2 Image Smoothing 25

3.2.1 Median Filter 25
3.2.2 Low-Pass Filter 26
3.3 Image Enhancement I - Inverse Filtering 28
3.3.1 What Is There and What Can Be Achieved 28
3.3.2 Linear Degradation Model 31
3.3.3 Inverse Filtering 33
3.3.4 Enhancement Filter Designing 34
Deriving the transfer function 35
Enhancement filter 36
3.4 Image Enhancement II - Intensity Modification 39
3.4.1 The Problems and Solutions 39
3.4.2 Global Intensity Modification 41
3.4.3 Local Intensity Correction 42
3.5 Image Segmentation 43
3.5.1 Regional Multi-Threshold Segmentation 43
3.5.2 Boundary Detection, Edge Sorting and Noise Removal 45
CHAPTER 4.EVALUATION 47
4.1 Phantom Studies - Transmission images 47
4.1.1 Study I - Uniformity Preservation vs. Boundary Distinguishability 50
4.1.2 Study II - Geometrical Information Study 52
4.2 Phantom Study - Attenuation Correction on Emission Data 54
4.3 Attenuation Correction Tool on Clinical PET Applications 57
CHAPTER 5.SOFTWARE DEVELOPMENT 59
5.1 Window System Programming Environment 59
5.1.1 The SunView Graphic User Interface 60
5.1.2 The Objects 61
Window objects 61
Other visual objects 62
5.1.3 The Notifiers 63
5.1.4 Color Table 65

5.2 General Flow of Control 66
5.2.1 Conventional Programming Flow Charts 67
5.2.2 Notification-Based Programming Structure 69
5.3 Using of Data Structure 72
5.3.1 "C" Data Types For Local Manipulations 73
5.3.2 SunView's Data Structure 75
5.4 Remote Procedure Calls 77
5.4.1 The RPC Model 78
5.4.2 Applications of RPC 80
CHAPTER 6.USER'S MANUAL 82
6.1 Getting Started 82
6.2 Loading Transmission Images 85
6.3 Displaying Images 86
6.3.1 Types of images to be displayed 86
6.3.2 Image displaying modes 87
6.3.3 Display handling menu 89
6.4 Enhancing Images 90
6.5 Edge Detection For Anatomic Segmentation 93
6.6 Interactive Boundary Repairing 96
6.6.1 General processing menu 97
6.6.2 Single edge handling menu 97
Changing the shape of selected boundary 99
Cutting and/or removing the edge segment 100
6.7 Attenuation Factor Map 101
6.8 Generating Attenuation Correction Sinogram 103
CHAPTER 7.SUMMARY 105
7.1 Conclusion of this project 105
7.1.1 Image processing approach 105
7.1.2 Interactive Drawing Package 106

7.1.3 Overall performance 107

7.2 Future Work 108

7.2.1 Second Thought On Current Work 108

7.2.2 Recommendation For Further Research 109

LIST OF REFERENCES 111

VITA 114

LIST OF FIGURES

Figure 2.1	Schematic representation of Compton scattering	10
Figure 2.2	Block Diagram of Adaptive Attenuation Correction Tool	19
Figure 3.1	Step.wise transmission image segmentation (Brain study I)	23
Figure 3.2	Step.wise transmission image segmentation (Brain study II)	24
Figure 3.3	Four Frames of CT Brain Images	29
Figure 3.4	Four Frames of PET Transmission Images	30
Figure 3.5	A model of image degrading process	31
Figure 3.6	Profile of a windowed inverse filter	37
Figure 3.7	A One.Dimensional Profile of the Inverse filter	38
Figure 3.8	A 3.D Surface Plot of a filtered image	40
Figure 3.9	Images before and after Intensity Modification	41
Figure 4.1	Uniform Cylinder Phantom Transmission Scan Images (Part I)	48
Figure 4.2	Uniform Cylinder Phantom Transmission Scan Images (Part II)	49
Figure 4.3	Emission Images with different Attenuation Correction Sinograms	56
Figure 4.4	Emission Images after/before attenuation correction using AACT	58
Figure 5.1	Control structures of two types of system	64
Figure 5.2	General flow of control of the AACT	68
Figure 5.3	Structure of the AACT	71
Figure 5.4	Application of Client Data	74

Figure 5.5 Remote Procedure Call Model 79

Figure 6.1 The Adaptive Attenuation Correction Tool (main window) 83

Figure 6.2 Filer and Colortool (Courtesy of CTI, Inc.) 84

Figure 6.3 Display Button's Pull.Right Menu With Display Options 87

Figure 6.4 Image Display Handling Menus 88

Figure 6.5 Image Enhancement Panel 91

Figure 6.6 Pop.Up Window for interactive options 94

Figure 6.7 Pop.Up Panel for Automatic Segmentation 95

Figure 6.8 General Purpose Menu On Interactive Window Canvas 98

Figure 6.9 Piecewise Handling Menu 98

Figure 6.10 Attenuation Factor Map with Attenuation Factor Menu 102

LIST OF TABELS

Table 3.1	A Two-Dimensional Spatial Smoothing Filter	27
Table 4.1	Scan Time (minutes) vs. Total Counts	47
Table 4.2	Noise Analysis on Phantom Transmission Studies (Original)	51
Table 4.3	Noise Analysis on Phantom Transmission Studies (Processed)	51
Table 4.4	Boundary Distinguishability on Phantom Study	52
Table 4.5	Diameter Measurement of Phantom before/after enhancement	53
Table 4.6	Emission Phantom Image Quality Analysis	55

CHAPTER 1. INTRODUCTION

1.1 Scope of Project

Medical care has been greatly enhanced by the invention of advanced medical imaging technology such as X-Ray Computed Tomography (CT) and Magnetic Resonance Imaging (MRI). These techniques can provide cross-sectional images of the anatomy of an internal body organ, e.g., heart and brain, without any surgical operation. These images can provide useful diagnostic information.

Positron Emission Tomography (PET) [1] is a relatively new imaging technique developed to fit the needs of revealing chemical and metabolic information about tissues and identify patterns of chemical changes in the diseases. It has similarities to CT and MRI in nature of scanning and image reconstruction. Because PET uses organic compounds which incorporate positron emitting isotopes as tracers, it can provide unique biochemical and physiologic information not obtainable through other imaging techniques for treatment of multitude of different diseases.

Until recently, only a few university medical research centers in the United States had performed PET imaging research. Due to the complex technical difficulties with routine PET imaging, such as the requirement of on-site cyclotron, the clinical utility of PET is just beginning to be realized. In January 1988, The University of Tennessee Medical Center at Knoxville (UTMCK) established a clinical PET facility.

By the end of June 1991, the PET center had two PET scanners and a cyclotron, built by Siemens/CTI, Inc. of Knoxville, Tennessee, which are used in daily clinical PET imaging. The intent of the center has been to provide clinical PET imaging for routine diagnosis and treatment and to conduct research for quantitative PET studies.

Attenuation phenomena [2] are major quality problems in quantitative PET imaging. The accuracy of data recovery from PET (quantitative PET) depends on correction for attenuation of the emitted photons within body. This project is designed to solve the attenuation problem by providing a complete, effective attenuation correction tool for routine clinical use.

1.2 Statement of Problem

Design improvements in instrumentation for Positron Emission Tomography have resulted in higher sensitivity and resolution, and potentially, the capability of more accurate quantitative measurements [3]. As applications of PET for studies of pathology and physiology become more sophisticated, the accuracy requirements in quantitative measurements also become more demanding. Because of these factors, it is overwhelmingly necessary to overcome one of the biggest enemies of quantitative

PET, the attenuation problem [1]. The Adaptive Attenuation Correction Tool developed in this project dedicated to solving this problem.

Photon attenuation is caused by the nonuniform absorption and scattering of tissues. Photons with different energy levels are attenuated differently for different types of tissue (attenuation mediums). Measures of the degree of attenuation by tissue are defined by the medium's attenuation factors, which can be used to estimate attenuation correction factors [1].

The correction of photon attenuation is normally based on the mathematical model of a band-limited distribution of emission detected with finite width detectors [1]. The application of this mathematical model is to create an attenuation correction factor map of each emission scan based on the corresponding attenuation mediums and generate a sinogram by calculating the exponential of the map's line integral. Next, this sinogram, called the attenuation correction factor (ACF) sinogram, is used to correct the sinogram emission scan and to reconstruct an attenuation correct emission image.

There are basically two practical methods to generate the ACF map [1], either by direct measurement of attenuation with external positron sources or calculations from simple geometric shapes that approximate the attenuation mediums. Both methods have their advantages and disadvantages. The transmission measurement method acquires the ACF sinogram by taking a transmission scans with external positron sources. Theoretically, this method can get the actual ACF sinogram from the attenuation medium and is very accurate. But transmission images have serious problems with random noise. Although noise levels can be decreased in various ways, like longer acquisition time, stronger external positron sources and even filters on the projection data, the amount of noise reduction is limited in relation to the price (in terms of time, degree of resulting images' distortion, etc.) paid for these efforts.

The geometric shapes method uses predefined geometric attenuation maps approximating certain parts of the patient's body (attenuation medium). Therefore, ACF sinograms can be calculated directly from these models. Usually these shapes consist of a set of ellipses simulating the tomographic shapes of body organs. The geometric shapes method is fast to process, especially with no transmission scan acquisition. However the direct use of this method has been gradually abandoned because it lacks the accuracy of approximation and predictability of the attenuation medium's actual shape.

Meanwhile, both the direct measurement method and geometric shapes method should also consider the effects of inaccurate attenuation correction from many other sources, like the degree of approximation of attenuation distribution function, width of detectors, mismatch of medium and statistical noise of ACFs. It is impossible to solve them all though. Nevertheless, the more factors which are considered and resolved, the more accurate the measurement.

1.3 Rationale of the Project

The Adaptive Attenuation Correction Tool (AACT) was developed to provide a comprehensive method which combines the advantages of the conventional methods with the intuition of human knowledge. The Adaptive Attenuation Correction Tool uses the methods of transmission measurement for acquiring basic information about attenuation media while using means of geometric measurements to generate accurate attenuation coefficient sinograms. A boundary detecting package is used first to provide key features of attenuation in the cross-sections of interest, and noise free transmission images are formed from these features. In practice, occasional distortion of transmission image features result in distortions from the actual shape of the attenuation medium. Therefore, a complimentary package is also provided for shape restoration. This package includes interactive boundaries correction, so that those boundaries with serious distortions are redrawn by the user. Thus, the ACFs are generated noise-free and anatomically correct.

Although the solution provided here is not sophisticated, especially considering the theoretic limitation of attenuation correction methods, this tool provides the potential of using a much shorter transmission scan time (see Chapter 4) to achieve competitive quality of attenuation correction against conventional methods. There are two major advantages of AACT vs. other methods described in Section 2.3. First, AACT is a complete, user-friendly operating tool which provides both sophisticated image processing procedures and user-interactive ability. Second, AACT uses much shorter transmission scan (5 minutes) images than all the other methods. In case of absence of transmission scan, AACT can still generate high quality attenuation correction factor sinograms from the emission scan images without attenuation correction (see Chapter 4).

The tool utilizes the SunView Window System and runs on SUN Workstations. The tool also runs in cooperation with some of the CTI's image tools, such as "Colortool" and "Filer" for users' convenience and system unity. A general operation procedure on the attenuation correction tool has following steps:

1. import transmission images
2. enhance images
3. detect automatic boundary
4. redraw boundary contour
5. map attenuation factors
6. calculate ACF sinograms

The reconstructions of transmission images and emission images are not included in this tool. Since the input and output of this tool are both standard PET files with matrix format, final reconstruction of image data can be performed by CTI software.

1.4 Outline of the Thesis

This thesis is composed of three related sections, each part has its own topic and consists of one or two chapters. Part I provides basic information. Part II discusses algorithms of transmission image processing and methods of interactive boundary redrawing. Part III talks about the practical implementation and realization of this project, including programming techniques and the procedures for operating this tool.

The purpose of Part I is to provide the background knowledge for this research, the problem definition, and the general approach toward the solution of the problem. Chapter 2 explains the nature of attenuation problems and briefly reviews the methods developed for attenuation correction. A brief introduction to the product of AACT is also given.

Part II is devoted to theory of image processing algorithms which were implemented in AACT. In Chapter 3, the discussion focuses on procedures of enhancement, segmentation and edge detection. The evaluation of the result is also provided in Chapter 4.

Part III, Practical Implementation covers two topics: programming techniques and the user's manual for the tool. In Chapter 5, several software development techniques involved in this tool are briefly introduced, the flow chart of the entire tool is sketched and data structure is also discussed. Chapter 6 is dedicated to an operation manual of the Adaptive Attenuation Correction Tool.

Finally, conclusions and some suggestions for the future work are provided in Chapter 7.

CHAPTER 2. METHODOLOGY

2.1 Nature of Problem

Positron Emission Tomography is a technique that not only delineates the internal structures of human body, but also measures the concentrations of positron-emitting radioisotopes within a three-dimensional object by the use of external measurements of the radiation from these isotopes. Those emitted photons from the annihilation of electrons and positrons pass through the tissue before hitting the detectors.

Attenuation [1] is defined as the scattering of these emitted photons away from their true course due to interaction with matter, therefore reducing the number of photons detected by the PET machine. This scattering is a function of the shape and density of the attenuating medium, which, if known, can be used to correct for the attenuation.

2.1.1 Basic Principles of PET

Positron Emission Tomography generates images by detecting and locating positron emitters which are used as tracers that are annihilating inside the patient's body. Proton-rich radioisotopes have two means of decay that will reduce excess positive charge on the nucleus [3]: (a) the nucleus can capture an orbital electron and neutralize positive charge with the negative charge of electron, or (b) a positive electron (a positron) can be emitted from the nucleus. The positron is an antielectron that, after traveling a short distance, will combine with electron from the surroundings and annihilate. On annihilation, the masses of both electron and positron are converted to electromagnetic radiation, which is in the form of two gamma rays of equal energy and emitted 180^{o} degrees from each other. It is the annihilation radiation that can be detected externally and is used to measure both the quantity and the location of the positron emitter [1].

The external detection and localization of a positron emitter inside an object takes advantage not only of the fact that two annihilation photons are emitted at 180^{o} to each other, but also of the fact that they are created simultaneously. In other words, the basic principle of coincidence detection is to use two opposing detectors in order to detect photons. The dual-detector system records annihilations by detecting the coincident events. If only one of the photons is detected, the event is rejected. A ring of detectors around a body detects annihilations from whole angles and reconstructs them back to a 2-D image.

2.1.2 Interaction Between Photons and Matter

Annihilation photons are high-energy photons. They transfer their energy to matter in complex interactions with atoms, nuclei and electrons. All these interactions can be considered as simple “collisions” between a photon and a target atom, nucleus, or electron. There are nine possible interactions between photons and matter [3], of which only five are of significance to nuclear medicine. And only one of those significant five is predominately related to the cause of the attenuation problem, and this is *Compton Scattering.*

Compton Scattering is a collision between a photon and a loosely bound outer shell orbital electron of an atom. Because the incident photon energy greatly exceeds the binding energy of the electron to the atom, the interaction looks like a collision between the photon and a "free" electron (Figure 2.1).

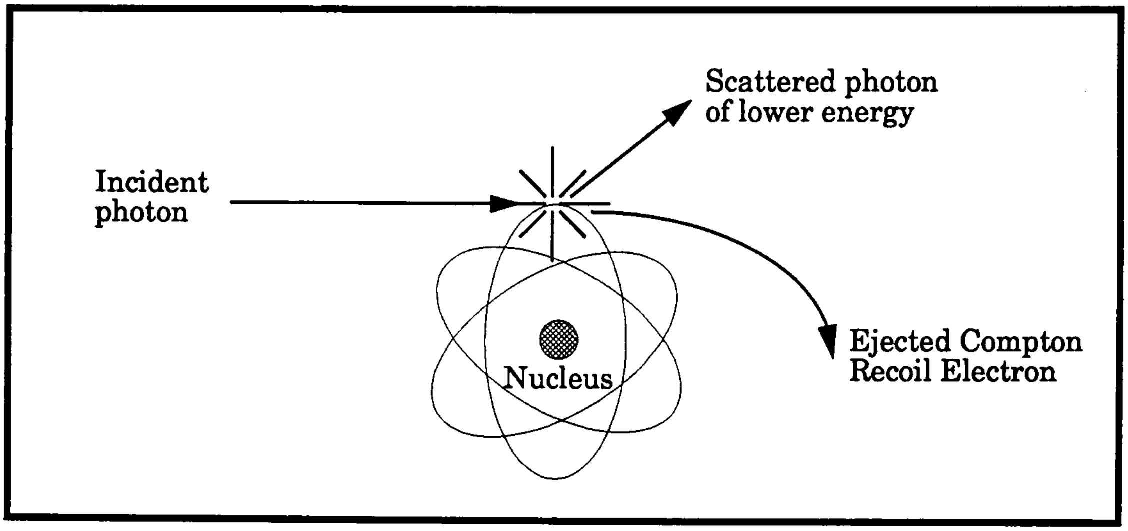

Figure 2.1 Schematic representation of Compton scattering

After collision, part of the photon energy is passed to the hit electron, which is called the *recoil electron*, and the photon with remaining energy is deflected through a scattering angle θ. The energy of the scattered photon is related to the scattering angle θ by considerations of energy and momentum conservation according to

$$E_{sc} = E_0 / [1 + (E_0/0.511)\,(1 - \cos\theta)] \qquad (2.1)$$

where E_0 and E_{sc} are the incident and scattered photon energies in MeV, respectively. The energy of the recoil electron, E_{re} is thus

$$E_{re} = E_0 - E_{sc} \tag{2.2}$$

The energy transferred does not depend on the density, atomic number, or any other property of absorbing material. Compton scattering is strictly a photon-electron interaction.

For the annihilation photon with 511 keV, the minimum energy of the scattered photon is E_{re} = 170 keV, and the angular distribution tends to be between 90° to 180°.

2.1.3 Attenuation of the Annihilation Photons

The manner in which annihilation photons are attenuated in coincidence detection is one of the attractive features of PET. In order for a coincidence event to be detected, both annihilation photons must be detected. Assuming that the linear attenuation coefficient (μ) is constant, the probability that the two photons will exit the body is given by

$$P_{12} = e^{-\mu a - \mu b} = e^{-\mu D} \tag{2.3}$$

where

a = Distance from source to edge of body for photon a,
b = Distance from source to edge of body for photon b,
D = Thickness of body.

This relationship means that the attenuation of coincident photons is independent of position between detectors. However, this implies that it is dependent on the thickness of the body. The matter of the body is not made uniformly of a single kind of tissue, thus the (μ) is no longer a constant, instead, it is a function of a and b, or simply D. The physical explanation of attenuation's position independence is due to the fact that both photons from one annihilation must be detected for a coincident event, and therefore the absorption path length is always the full thickness of the attenuating medium.

2.1.4 Mathematical Correction of Attenuation

In practice, the attenuation problem is corrected in the process of back projection by using attenuation correction factors [1] [2].

Equation (2.4) is an expansion formula of Equation (2.3). Equation (2.4) shows the use of attenuation correction factors in the back-projection procedure for generating an attenuation corrected sinogram.

$$\begin{aligned} P_{\gamma\gamma}(\xi, \theta) &= exp\,[-\iint \mu\,(x,y)\,K\,(\xi, \theta, x, y)\,dxdy] \\ &\quad \times \iint \rho\,(x,y)\,K\,(\xi, \theta, x, y)\,dxdy, \end{aligned} \tag{2.4}$$

here, $P_{\gamma\gamma}(\xi, \theta)$ is the photon emission projection data (the original sinogram from the transmission scan) collected by the detector at projection angle θ and projection beam number ξ; $K(\xi, \theta, x, y)$ is the geometric function which defines the course of projection, $K = 1$ if the projection beam ξ with angle θ passes through point (x, y), and $K = 0$ otherwise, $\mu\,(x, y)$ is the attenuation coefficient at this point (x, y). The part $exp\,[-\iint \mu\,(x,y)\,K\,(\xi, \theta, x, y)\,dxdy]$ is thus the attenuation factor value at projection angle θ and beam number ξ. $\rho(x, y)$ is the true density distribution of emission data at (x, y), and $\iint \rho(x, y) K(\xi, \theta, x, y)\, dxdy$ is the true projection data which is expected after the attenuation correction. The Attenuation Correction Tool is for the purpose of generating geometrically correct, noise-free attenuation coefficient $\mu(x, y)$.

2.2 Corrections for Attenuation

In the actual PET system, $\mu(x, y)$ represents a transmission image generated from the back-projection of sinogram $\iint \mu(x, y) K(\xi, \theta, x, y)\, dxdy$. This sinogram is obtained by using an external positron emitting source to determine the attenuation of the body according to Equation 2.3. $P_{\gamma\gamma}(\xi, \theta)$ is the emission sinogram. The collection of $\rho(x, y)$ is the attenuation corrected emission image.

There are two basic methods [1] for attenuation correction: *calculated attenuation correction* and *measured attenuation correction.*

2.2.1 Calculated Attenuation Correction

Calculated Attenuation Correction uses geometric shapes to simulate an actual attenuation coefficient map. If the value of the μ is constant and the shape and location of the cross section are known, this method allows accurate and easy evaluation of the attenuation correction to enable quantitative PET measurement. In several areas of the body, such as the brain and torso below the thorax, this method provides a reasonable estimation of the attenuation.

The attractions of the calculated attenuation correction method, even in the body where it is not exact, are

1. the ease of application;
2. elimination of the need to do additional measurements of the actual attenuation factor map (a transmission scan);
3. elimination of the need to have the patient in exactly the same position for both emission and transmission PET scan;
4. elimination of propagation of statistical error from the additional measurements.

With a PET system that has the appropriate hardware and software, the edge of the body can easily be estimated from an emission scan reconstructed from the uncorrected data. This gives both position and size of the cross-section, and the calculation is straightforward.

The disadvantages of this method are also obvious:

1. No part of body has constant attenuation, and the regions containing air and bone can cause significant error in quantization, especially in areas adjacent to such structures.
2. The shape of the body part is difficult to define exactly, and errors in position and size of a centimeter or more can be easily made, which can be critical for structures near the outside edge of the body.
3. It is impossible to use with any validity in thorax because of the large size of the lungs, which have an attenuation coefficient about one third that of the surrounding tissue.

2.2.2 Measured Attenuation Correction

As mentioned before, the attenuation is independent of the position between detectors. Thus, by placing the ring source around a patient's body prior to injection of a positron emitting tracer, and have the annihilating photons detected coincidence, the data provides a measure of the actual attenuation in cross-section. This measurement is called a transmission scan rather than an emission scan.

The primary advantage of the measured attenuation correction over the calculated method is that it is a measure of the attenuation properties of the actual object. But the disadvantages are also considerable:

1. It requires an additional measurement;
2. The patient must remain in or be repositioned in the exact same place for the emission study;
3. The propagation of the statistical error from the attenuation measurement to the final image data may be significant.

Despite these disadvantages, the measured attenuation method is still the main stream for attenuation correction. The reason is obvious. The calculated method cannot predict the variety of a patient's body and his/her corresponding attenuation exactly; however, the measured method through certain image processing techniques can restore the actual attenuation of body. Thus the measured method provides accurate attenuation correction for quantization of PET.

2.2.3 Combined Measured and Calculated Attenuation Correction

By combining two methods, as one can see from the above discussion, it is possible to obtain the benefits of both the measured and calculated attenuation correction methods while minimizing their disadvantages. An approach has been proposed to do short, low-counts scans for transmission images and extract the shapes and positions of the major attenuation medias. Each region of attenuation media is assigned an appropriate attenuation coefficient and the attenuation correction factors sinogram is forward projected from this attenuation coefficients map. This method removes the statistical errors of the measured correction, while retaining the major detail of the structures.

2.3 Review of Previous Works

There are a few works concerning this problem in the past decade, since the calculated method has gradually been abandoned due to its limitation, and the majority of PET users utilize the measured attenuation correction method.

In 1981, Huang *et al* [4] introduced an attenuation correction method based on boundary detection and segmentation. The method used PET's transmission image as a working object. The transmission image was modified with two-dimensional smoothing technique, by iteratively convolving with a 5 by 5 smoothing filter to removed statical noise. Therefore, boundaries between regions with significant differences in attenuation were either drawn with a joy-stick interfaced to the video display unit or be allocated by an edge-finding computer program in order to reduce the amount on operator interaction and the dependence of operator judgement. The edge-finding program was subdivided into two parts: *edge enhancement* by a four-pixel Laplacian Operator and *edge tracing* picking up the single-pixel-width edge with minimum Laplacian value.

In 1982, Bergström *et al* [5] introduced another contour-finding algorithm, which outlined the periphery of an object in a PET scan by placing point sources all around the skull to allocate the actual boundary of the bones. The method provided an accurate contour of the brain, and thus greatly reduced errors which occurred around high attenuation coefficient regions like bone.

In, 1990, Ganti *et al* [6] presented a multi-resolution pyramid technique attenuation correction. Each level above the base level is a lower resolution version of its predecessor image. A histogram based region merging was done to extract the desired number of homogeneous regions The segmented transmission images are used to compute the computes the attenuation correction factors.

In, 1990, Xu *et al* [7] introduced a more simplified scheme of segmentation-based attenuation correction. The regions are segmented by a spatial-domain statistic measurement -- intensity histogram. The mean of intensity within the regions are determined by peaks in the histogram and the thresholds which divides regions by the valley value on the histogram. The attenuation factors are also computed from the average value within each region.

2.4 The Adaptive Attenuation Correction Tool

The Adaptive Attenuation Correction Tool (AACT) hereby described uses the combined method. A short transmission scan is performed to provide the information of working object. The attenuation factor map is computed by segmenting the transmission PET image. The attenuation correction factor sinogram is computed by forward-projection of segmented transmission image (attenuation maps). The combination of these two processes gives fast and accurate attenuation correction with a powerful interactive capability. Finally, the emission PET scan is reconstructed by utilizing the attenuation correction factor sinogram to modify the emission projection data.

The adaptive attenuation correction tool in this project focuses on steps 2 and 3, since the first and last steps have already been built as basic functions for PET. Figure 2.2 is a block diagram that illustrates the procedures.

Chapter 3 will provide detail discussion about the algorithms implemented for the operations of the Adaptive Attenuation Correction Tool, their theoretical background, their advantages and disadvantages as well as their implementation in the project.

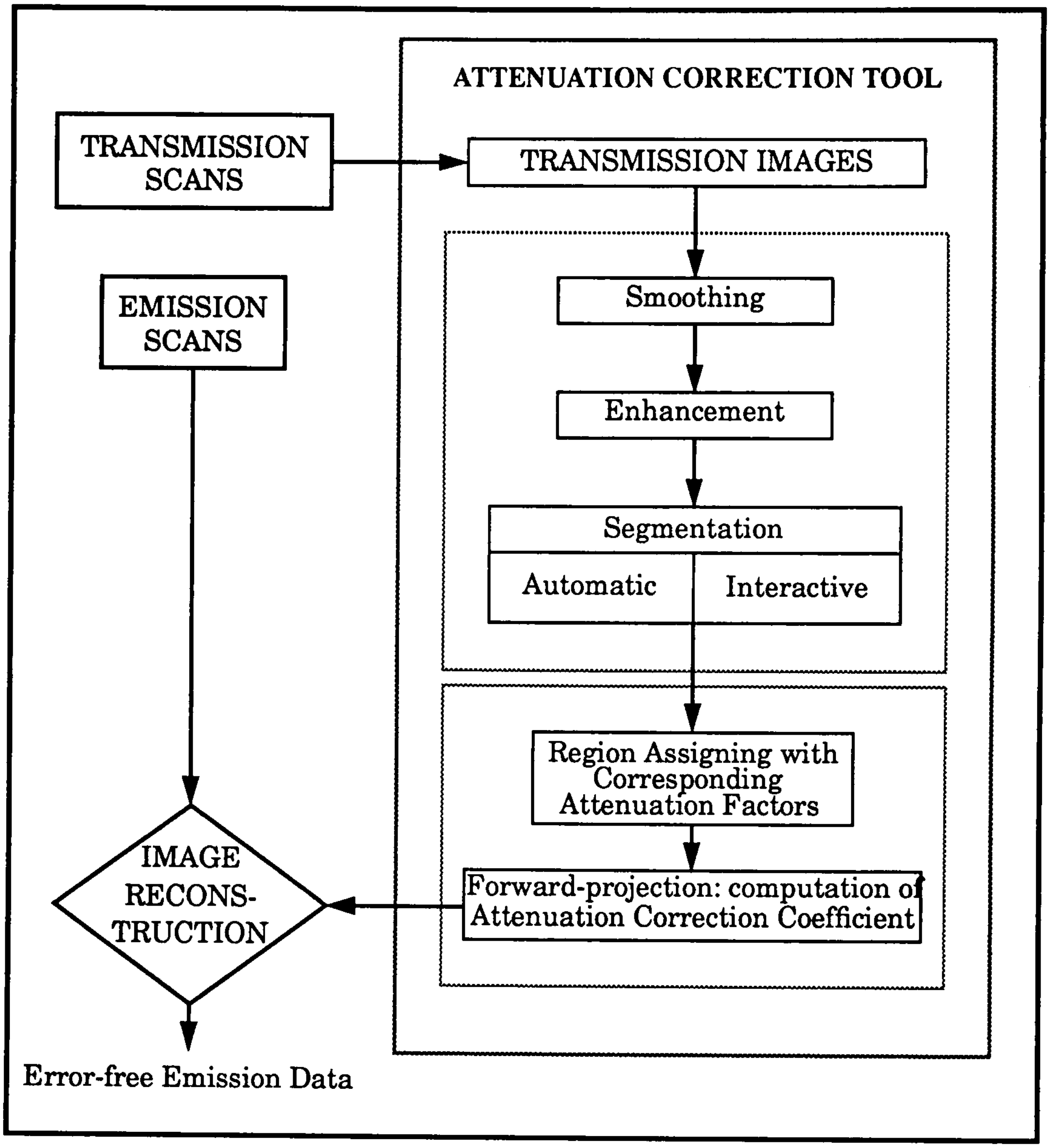

Figure 2.2 Block Diagram of Adaptive Attenuation Correction Tool

CHAPTER 3. IMAGE SEGMENTATION

The transmission images generated through external radioactivity suffer from low counts and limited spatial resolution. These problems are especially severe when a short transmission scan is used. The attenuation coefficient (μ) values in the transmission images are therefore quite inaccurate. That is also why a combination method is used; the shapes of attenuation matter must be restored through image processing and interactive drawing procedures, and each region of structure is assigned with its corresponding μ.

3.1 General Procedures

The process of generating a good quality attenuation coefficient map involves image processing. A transmission image is first restored and then segmented into regions of different anatomic structures. Finally, an attenuation coefficient map is generated according to the segmented transmission image. The μ values for each attenuation material used in this thesis were obtained from data published by McCullough [8]. In order to avoid inaccuracy, no μ values were assigned directly or indirectly from the transmission data. The attenuation correction sinogram is thus generated from the attenuation coefficient map by forward-projection and exponential calculation, and eventually used to correct the emission scan sinogram.

3.1.1 Dual Approach

Transmission image quality is corrupted due to low counts of detection, statistical noise, and system limitation (especially when a short transmission scan is used). Therefore, a scheme of interactive control of image processing based on the visual image quality became a part of the thesis. However, the project still emphasizes on the mathematical solution to maximize the efficiency of operation.

In AACT, the process of segmentation is broken into two totally different methods, *automatic segmentation* using a model-based image processing, and *interactive segmentation* offering a complete set of graphic options for drawing and redrawing boundaries. Furthermore, the interactive package is also designed to be used as a supplementary program to automatic segmentation.

3.1.2 Multi-Step Segmentation Scheme

Because of transmission images' noisy and non-uniform nature, the segmentation of transmission images is broken down into three major steps: *image smoothing*, *image enhancement*, and *boundary detection*. *Image smoothing* applies both a median filter and low-pass filter in the spatial domain of the transmission image to improve signal-to-noise ratio. *Image enhancement* increases image quality by revealing more boundary details with better segmented subregions. The enhancement uses the inverse filtering technique along with intensity modification. *Boundary detection* is the final step. It detects the boundary of each effective region, and removes noise and false contours. Each region will later be filled with a corresponding attenuation coefficient for computing the attenuation correction factors sinogram. Figure 3.1 and Figure 3.2 display two examples of brain transmission images to illustrate the image processing procedures implemented by AACT. In both figures, (a) is the original transmission image and (b) displays with an additional intensity profile, (c) and (d) are images after "windowed" inverse filtering and a modified inverse filtering, respectively, (e) is intensity modified version of (d), and (f) is the image with edge extraction.

3.1.3 Interactive Procedures

Although the attention of designing the Adaptive Attenuation Correction Tool has mostly focused on analytical approach and full automation, it is still very practical to take the advantage of human intuition, coupled with the versatility and high speed of automatic processing. There are two parts of interactive activity utilized in this tool, interactive process quality control and interactive segmentation (or edge drawing).

The interactive process quality control enables the user to monitor each step throughout the process of the tool. Each process displays intermediate result, and lets the operator determine the quality of process. Different parameters and options are also provided with each process for better quality output.

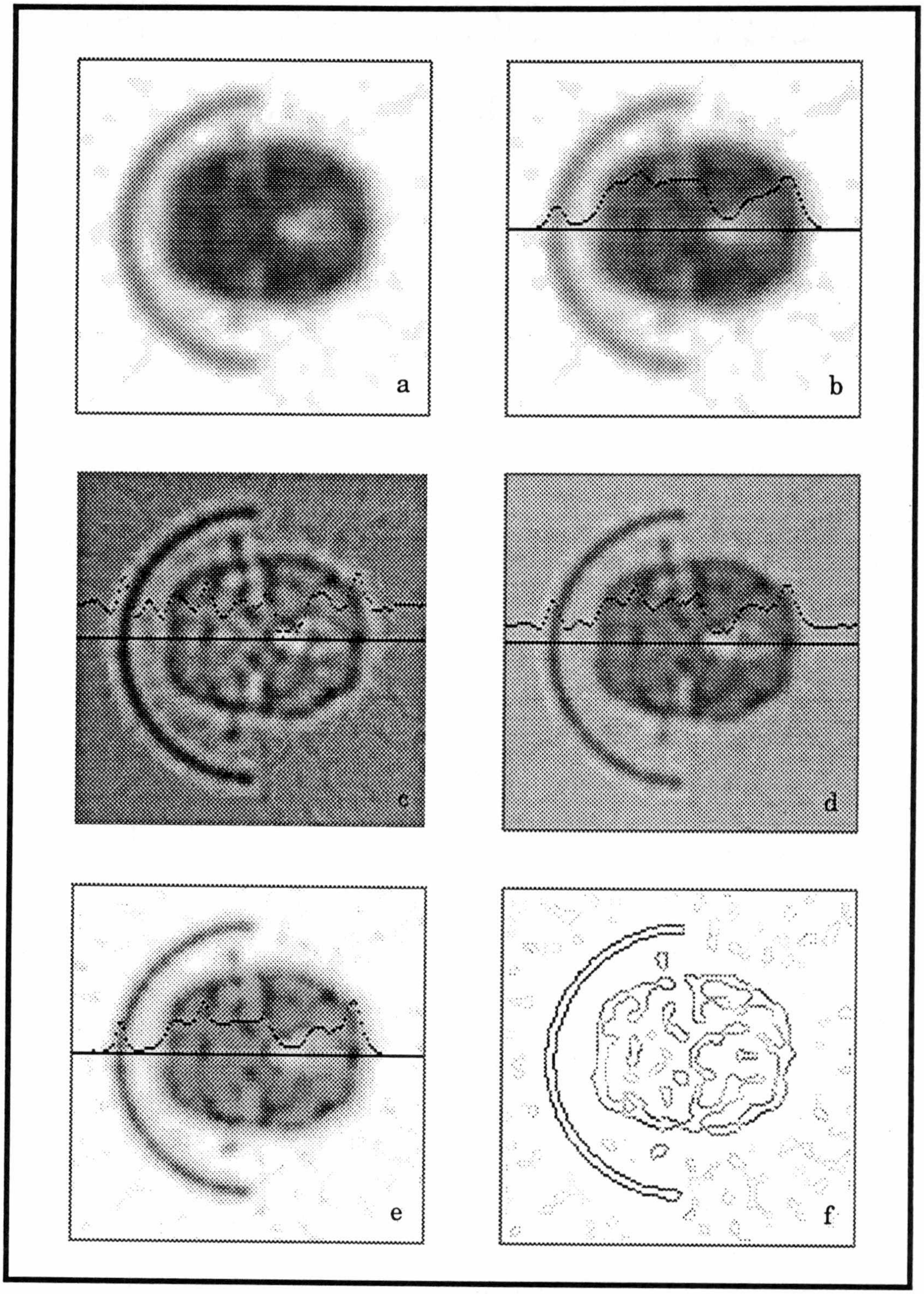

Figure 3.1 Step-wise transmission image segmentation (brain study I)

(Image IDs are correspondent to the explanation in Page 22)

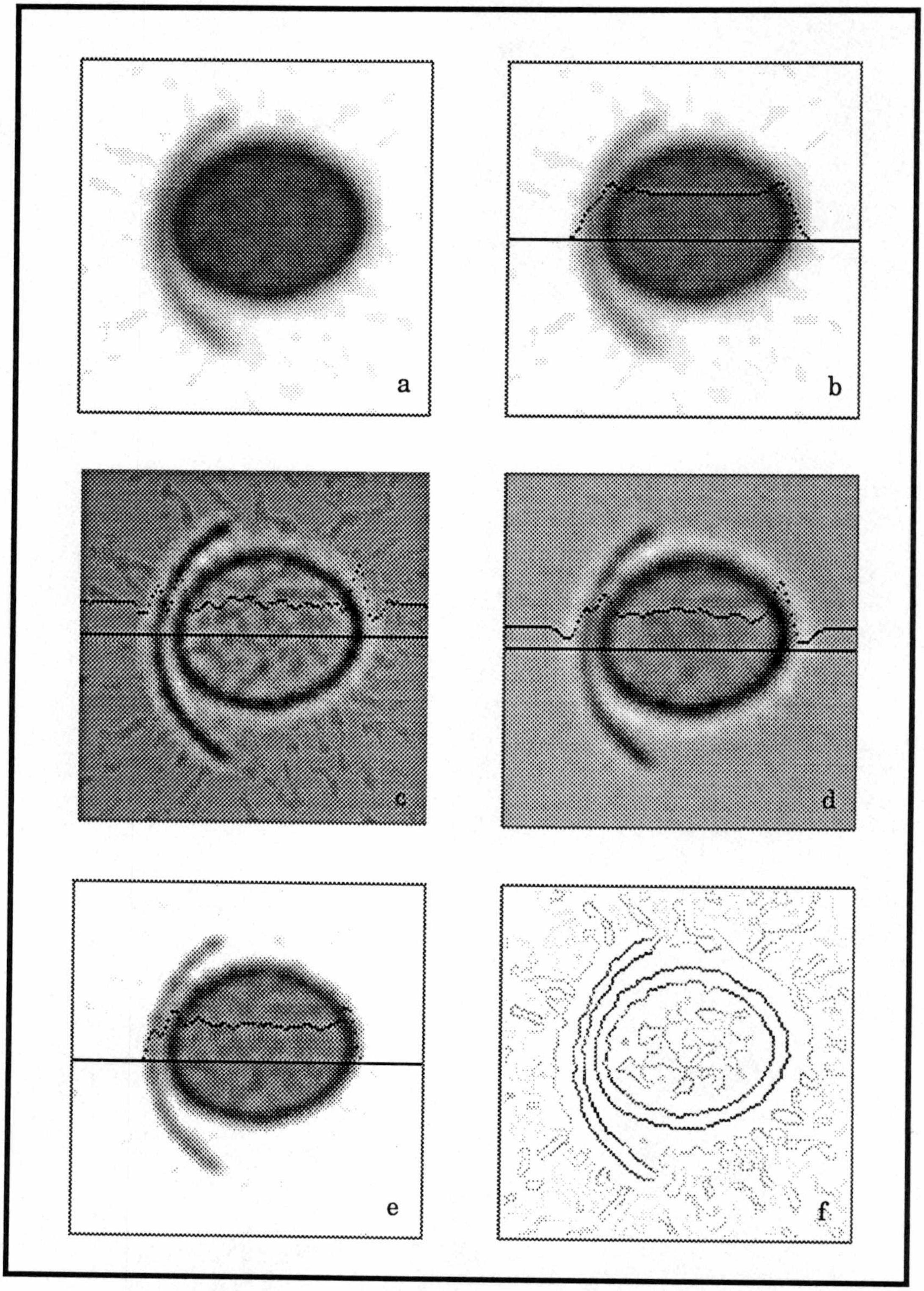

Figure 3.2 Step-wise transmission image segmentation (brain study 2)

(Image IDs are correspondent to the explanation in Page 22)

The interactive edge drawing package enables the user to either draw edges directly on the image, or adjust and alter the edges generated by automatic segmentation. The user can choose either one or both to ensure the best possible segmentation for computing the attenuation correction factors. This interactive package also includes options for the attenuation coefficient assignment.

A complete description on how to effectively use the interactive package is in Chapter 5.

3.2 Image Smoothing

Smoothing operations are used here for diminishing spurious effects in the transmission scan images as a result of poor photon sampling in the detecting system. In the Adaptive Attenuation Correction Tool, two types of image smoothing methods are used, a *median filter* and a *low-pass filter*, each serves for different purpose of smoothing.

3.2.1 Median Filter

The *median filter* [9] is chosen to pre-process the image, thus removing random noise contained in the transmission images [2] [10] [11]. This procedure results in a image with both higher signal-to-noise ratio and preserved edge information.

"The median m of a set of values is that half of the values in the set are less than m and half are greater than m." [9] For example, in a 5×5 neighborhood of a pixel the median is the 13th largest value. In order to perform the median filtering on a two-dimensional image, a pixel value is modified by the median of its neighborhood pixel values. The principal function of a median filter is to force pixels with very distinct intensities to be more like their neighbors, thus actually eliminating intensity spikes that appear isolated in the area of the filter mask.

3.2.2 Low-Pass Filter

Because the transmission image suffers from low-count radiation detection which causes low resolution and poor uniformity [12], a *low-pass filter* is also applied for smoothing image pixel values and increasing uniformity. This effect can not be achieved by median filtering.

The actually implementation of a low-pass filter in AACT is a spatial domain neighborhood averaging technique. *Center Weighted neighborhood average* [9] is a typical example used here. Table 3.1 shows a typical 11×11 mask (or weight map) generated by a Gaussian distribution function [13]. This mask is convolved with the image for smoothing. The bigger the mask size is, the smoother the result will be. However, wider margins remain unsmoothed, image gets more blurred and the calculation becomes more time-consuming.

Table 3.1: A Two-Dimensional Spatial Smoothing Filter, the mask size is 11×11

0.0014	0.0028	0.0041	0.0054	0.0069	0.0083	0.0069	0.0054	0.0041	0.0028	0.0014
0.0028	0.0055	0.0080	0.0105	0.0135	0.0165	0.0135	0.0105	0.0080	0.0055	0.0028
0.0041	0.0080	0.0128	0.0175	0.0233	0.0290	0.0233	0.0175	0.0128	0.0080	0.0041
0.0054	0.0105	0.0175	0.0245	0.0330	0.0415	0.0330	0.0245	0.0175	0.0105	0.0054
0.0069	0.0135	0.0233	0.0330	0.0431	0.0533	0.0431	0.0330	0.0233	0.0135	0.0069
0.0083	0.0165	0.0290	0.0415	0.0533	0.0650	0.0533	0.0415	0.0290	0.0165	0.0083
0.0069	0.0135	0.0233	0.0330	0.0431	0.0533	0.0431	0.0330	0.0233	0.0135	0.0069
0.0054	0.0105	0.0175	0.0245	0.0330	0.0415	0.0330	0.0245	0.0175	0.0105	0.0054
0.0041	0.0080	0.0128	0.0175	0.0233	0.0290	0.0233	0.0175	0.0128	0.0080	0.0041
0.0028	0.0055	0.0080	0.0105	0.0135	0.0165	0.0135	0.0105	0.0080	0.0055	0.0028
0.0014	0.0028	0.0041	0.0054	0.0069	0.0083	0.0069	0.0054	0.0041	0.0028	0.0014

Although low-pass filter will blur the image, with an appropriate low-pass filter, the gain from the increased uniformity is expected to be greater than its trade-off, degradation of edge information.

3.3 Image Enhancement I - Inverse Filtering

The quality of the transmission image is poor due to three major reasons, low resolution, scattered photons and non-uniformity of photon beams. Furthermore, the windowing process on the projection data reduces noise as well as sharp details. Therefore, the intensity of each pixel on the transmission image is no longer accurate, and the image needs to be enhanced.

3.3.1 What Is There and What Can Be Achieved

Transmission images are generated through an external positron source, either a ring source, a rod, sector source or rotating source containing long half-life isotope. This situation is quite similar to X-ray Computed Tomography (CT), and differs in practice due to differences in the detector systems. The only difference is that the energy level of γ-ray: x-ray is around 40 - 80 KeV with almost consistent emitting, and the annihilation of positron emits 511 KeV photons, and the PET suffers from low counts of photons [1] [3] [11] [12].

Low counts of photons has direct impact on the image quality. Compare the images in Figures 3.3 and 3.4, where two sets of typical images, each containing four frames of images, are taken by CT (GE 9800) and PET (Siemens/CTI ECAT 931) transmission scanners at the corresponding cross-sections. The difference of quality between a CT scan image and a PET transmission image are obvious. Achieving more structural information from PET transmission images is the task of Inverse Filtering.

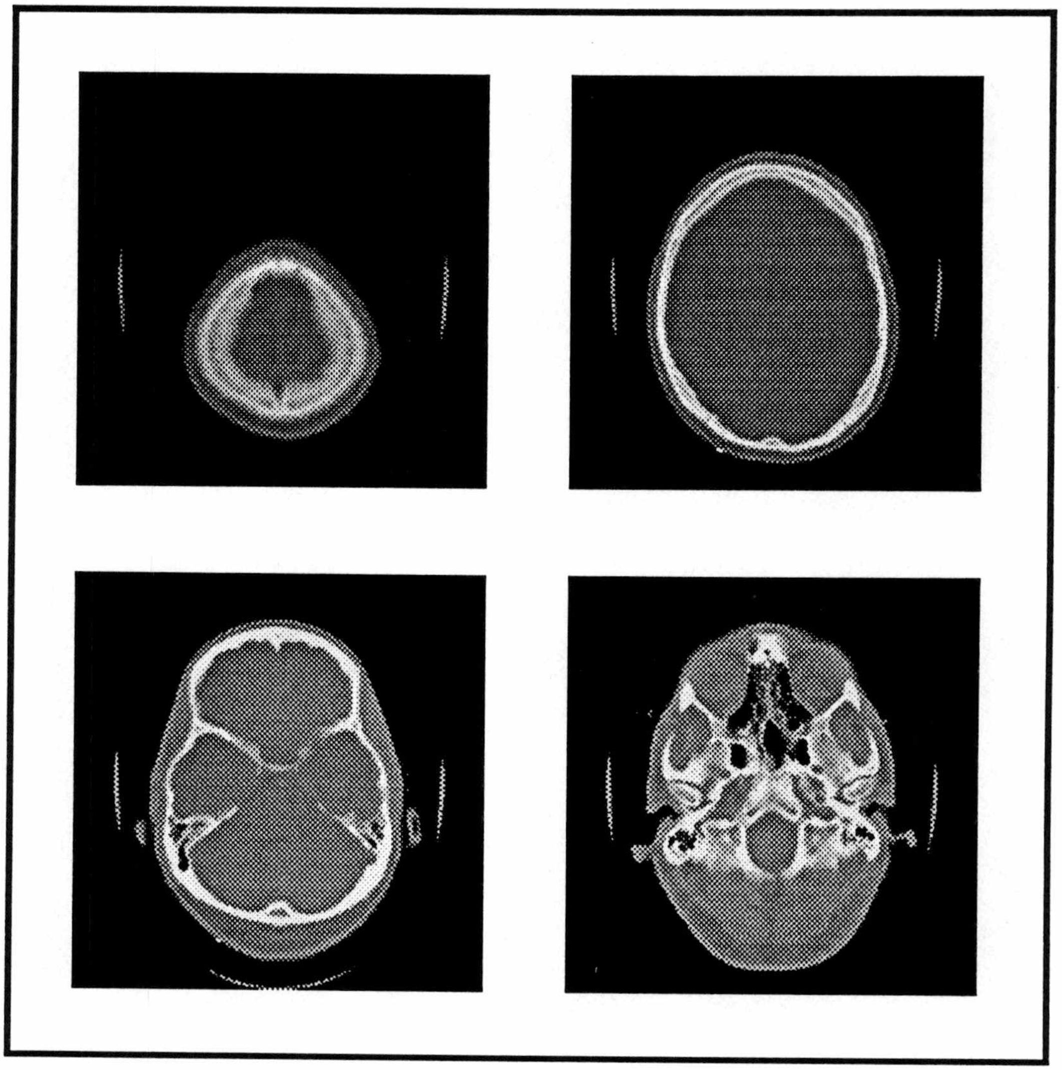

Figure 3.3 Four Frames of CT Brain Images

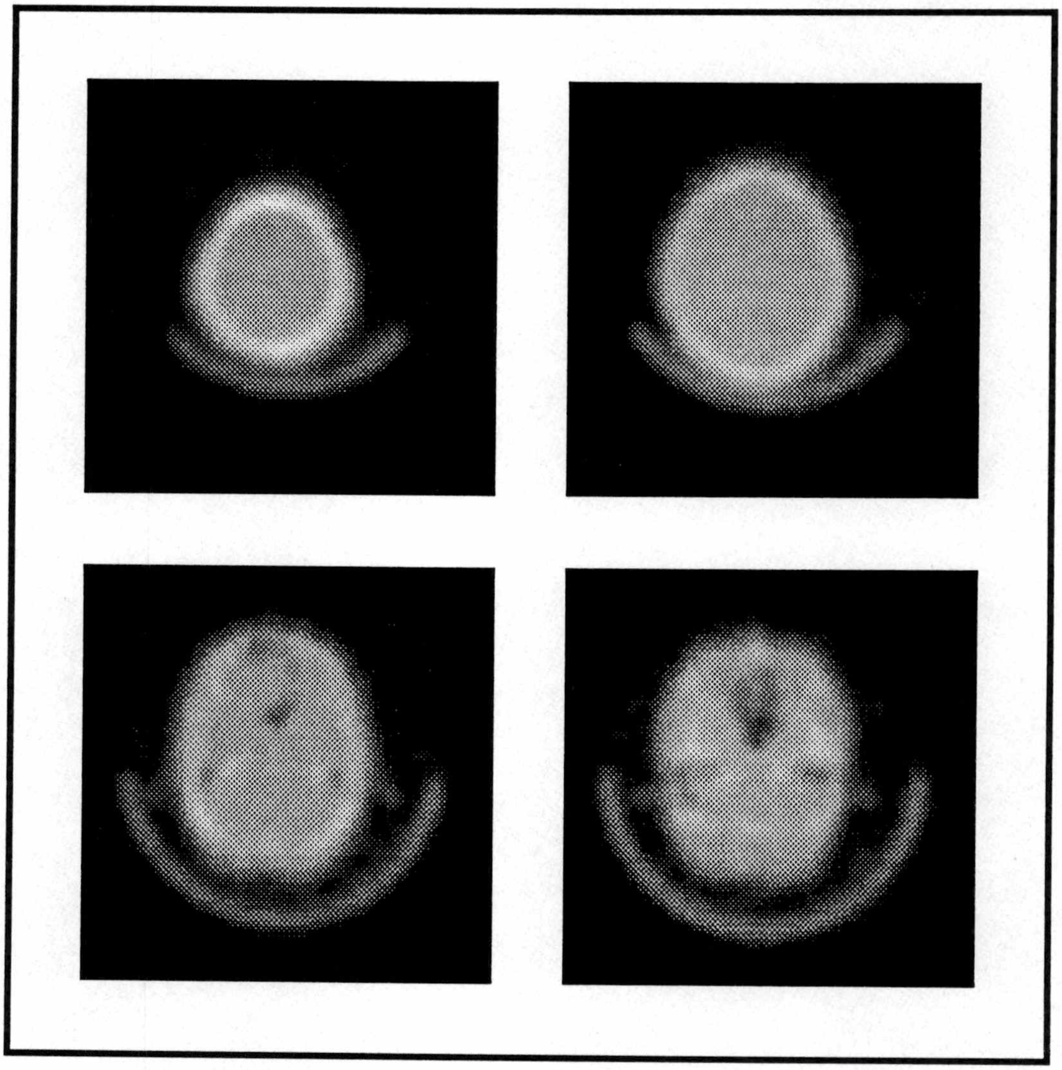

Figure 3.4 Four Frames of PET Transmission Images

3.3.2 Linear Degradation Model

As shown in Figure 3.5, a degradation system can be modeled as an operator (or system) H, which together with an additive noise term $\eta(x, y)$ operates on an input image $f(x, y)$ to produce a degraded image $g(x, y)$ [9] [13]. The image enhancement is thus viewed as that of obtaining an approximation to $f(x, y)$, given $g(x, y)$ and a knowledge of the degradation in the form of H, while the knowledge of $\eta(x, y)$ is limited to the information of a statistical nature.

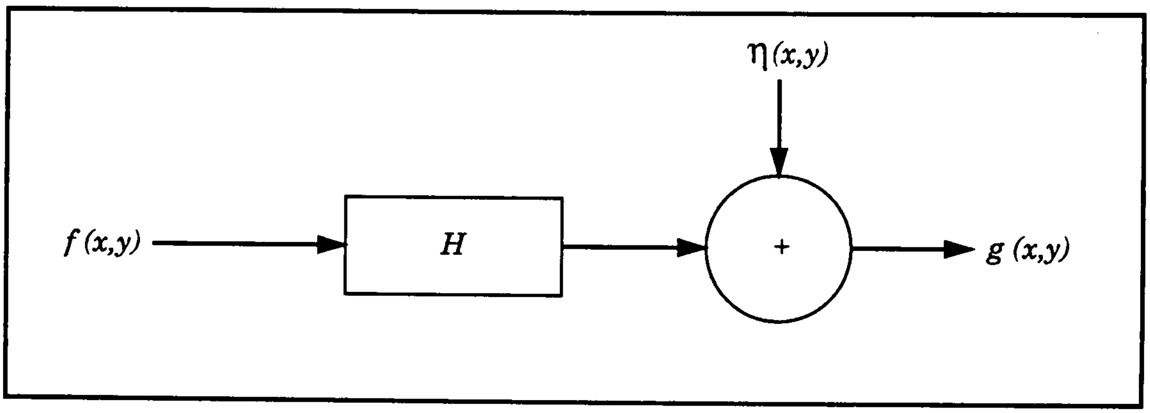

Figure 3.5 A model of image degrading process

The input-output relation in Figure 4.3 is given by the expression

$$g(x, y) = H(f(x, y)) + \eta(x, y). \tag{3.1}$$

From the definition of impulse function [9], $f(x, y)$ can be further expressed in the form

$$f(x, y) = \int_{-\infty}^{\infty}\int_{-\infty}^{\infty} f(\alpha, \beta)\,\delta(x - \alpha, y - \beta)\,d\alpha d\beta. \tag{3.2}$$

Then, if $\eta(x, y) = 0$ in Equation (3.2), with linear operator H, and input $f(\alpha, \beta)$ independent of x and y, and because of linear system's properties of additivity and homogeneity [14],

$$g(x, y) = \int_{-\infty}^{\infty}\int_{-\infty}^{\infty} Hf(\alpha, \beta)\, \delta(x-\alpha, y-\beta)\, d\alpha d\beta. \qquad (3.3)$$

The term

$$h(x, \alpha, y, \beta) = H\delta(x-\alpha, y-\beta) \qquad (3.4)$$

is called the *impulse response* of H. Here $h(x, \alpha, y, \beta)$ is the response of H to an impulse at coordinates (α, β), and commonly referred as the *point spread function.* Substitution of Equation (3.4) yields expression

$$g(x, y) = \int_{-\infty}^{\infty}\int_{-\infty}^{\infty} f(\alpha, \beta)\, h(x, \alpha, y, \beta)\, d\alpha d\beta, \qquad (3.5)$$

which is called the *superposition* (or *Fredholm*) *integral of the first kind.* From this expression, one can conclude that if the response of a linear system H to an impulse is known, then the response to any input $f(\alpha, \beta)$ can be calculated by using Equation (3.5).

Furthermore, to a position-invariant system H, $g(x, y)$ can be expressed as the result of convolution integral of $f(x, y)$ and $h(x, y)$, that is

$$g(x, y) = \int_{-\infty}^{\infty}\int_{-\infty}^{\infty} f(\alpha, \beta)\, h(x-\alpha, y-\beta)\, d\alpha d\beta. \qquad (3.6)$$

In the presence of additive, position-invariant noise, the expression describing a linear degradation model becomes

$$g(x,y) = \int_{-\infty}^{\infty}\int_{-\infty}^{\infty} f(\alpha,\beta)\, h(x-\alpha, y-\beta)\, d\alpha d\beta + \eta(x,y). \tag{3.7}$$

Although, in the real world, degradation systems are mostly non-linear, the linear approximation still has advantage, since such approaches make the extensive tools of linear system theory available for the solution of image-restoration problems; non-linear, space-variant techniques often have no known solution or are very difficult to solve computationally.

3.3.3 Inverse Filtering

From Equation (3.7), the actual image output corrupted by the degradation system $g(x,y)$ is the convolution integral of input image $f(x,y)$ and impulse response of the degradation system $h(x,y)$, plus additive noise. Thus, from the view of frequency domain, their relation is as follows,

$$G(u,v) = F(u,v)H(u,v) + N(u,v) \quad . \tag{3.8}$$

Here, $G(u,v)$, $F(u,v)$, $H(u,v)$, and $N(u,v)$ are the *Fourier* transform of $g(x,y)$, $f(x,y)$, $h(x,y)$ and $\eta(x,y)$, respectively. Therefore, the first thought about the inverse filtering is to rewrite Equation (3.8) into

$$F(u,v) = \frac{G(u,v) - N(u,v)}{H(u,v)}, \tag{3.9}$$

or

$$F(u,v) = \frac{G(u,v)}{H(u,v)} - \frac{N(u,v)}{H(u,v)}, \tag{3.10}$$

and $f(x,y)$ can then be computed by the inverse *Fourier* transform.

Equation (3.9) is a perfect theoretical solution which can hardly be matched in practice. Especially if $H(u, v)$ is zero or very small, the fraction $\frac{N(u, v)}{H(u, v)}$ dominates the restoration result. This is very possible in practice, because $H(u, v)$ drops off rapidly as a function of distance from the original of uv plane (frequency domain), while the noise term normally drops off much slower.

A general approach for resolving these problems is achieved in two ways: image smoothing to minimize the standard deviation of noise distribution, and choosing a small neighborhood from the original of uv plane to avoid a small value for $H(u, v)$ [9]. Therefore, the resulting image $f(x, y)$ can be obtained with less influence from the fraction $\frac{N(u, v)}{H(u, v)}$.

3.3.4 Enhancement Filter Designing

The enhancement filter is designed based on the modification of inverse filtering. The practical designing includes some assumptions and understanding of the image, since the distortion information is not complete. These assumption and understandings are: (1) the information about image noise distribution is not complete and accurate, (2) the processing time must be short enough so that daily clinical operation is feasible, and (3) a complete restoration is impossible anyway. The interactive package is an essential backup when there is no computable solution for enhancement exists.

Enhancement filter designing has two steps: inverse filtering and modification. Inverse filtering generates a filter profile based on the simulated noise model;

modification procedure then modifies the inverse filter into a practical filter. The second step also includes a lot of testing on real transmission images.

3.3.4.1 Deriving the transfer function

On the other hand, inverse filtering procedure using Equation (3.10) with the noise effect ignored may have a different emphasis from what is expressed above, assuming the major distortion of a collimated photon beam is caused from scattering [3] [11]. This out-of-focus phenomena is presented as a spill-over effect. If the spill-over effect is expressed by a bell-shaped curve, as in the projection data from a point source, then the probability of a detector seeing an event is

$$P_c = 1 - \frac{1}{\sqrt{2\pi}\sigma} e^{-\frac{x^2}{2\sigma^2}}, \tag{3.11}$$

where x is the distance of detectors from center, and σ is the standard deviation while the mean of distance is zero. Equation (3.11) is expressed based on the assumption that the matter is uniform in density, there is no photon deflected into other cross-sections or projection planes, and no photon is absorbed by the matter, so that Equation (3.11) should satisfy

$$\int_{-\infty}^{\infty} P_c dx = \int_{-\infty}^{\infty} \frac{1}{\sqrt{2\pi}\sigma} e^{-\frac{x^2}{2\sigma^2}} dx = 1. \tag{3.12}$$

With back-projection, the noise distribution on a two-dimensional image is expressed as following,

$$P_c = 1 - \frac{1}{2\pi\sigma^2} e^{-\frac{x^2+y^2}{2\sigma^2}} \quad , \qquad (3.13)$$

here, σ remains the same in either direction (x or y) since σ is from one dimensional projection. Furthermore, the impulse function of a point of transmission matter scanned by external photons is expressed as

$$h(x, \alpha, y, \beta) = \frac{1}{2\pi\sigma^2} e^{-\frac{(x-\alpha)^2+(y-\beta)^2}{2\sigma^2}} \quad . \qquad (3.14)$$

3.3.4.2 The enhancement filter

From Equation (3.14) transfer function is therefore derived by two-dimensional Fourier transform as

$$H(u, v) = e^{-2\pi^2\sigma^2(u^2+v^2)} . \qquad (3.15)$$

The direct inverse filter is thus derived as

$$H(u, v) = e^{2\pi^2\sigma^2(u^2+v^2)} \qquad (3.16)$$

A filter transfer function like Equation (3.16) magnifies high frequency components quickly as the distance from the origin getting larger (see Figure 3.16). On the other hand, the distortion from fraction $\frac{N(u, v)}{H(u, v)}$ in Equation (3.10) at higher frequency will be extremely severe. It is necessary to “window” the filter in Equation (3.16) by choosing a small neighborhood around the origin of uv plane (Figure 3.6) and “flat out” the rest.

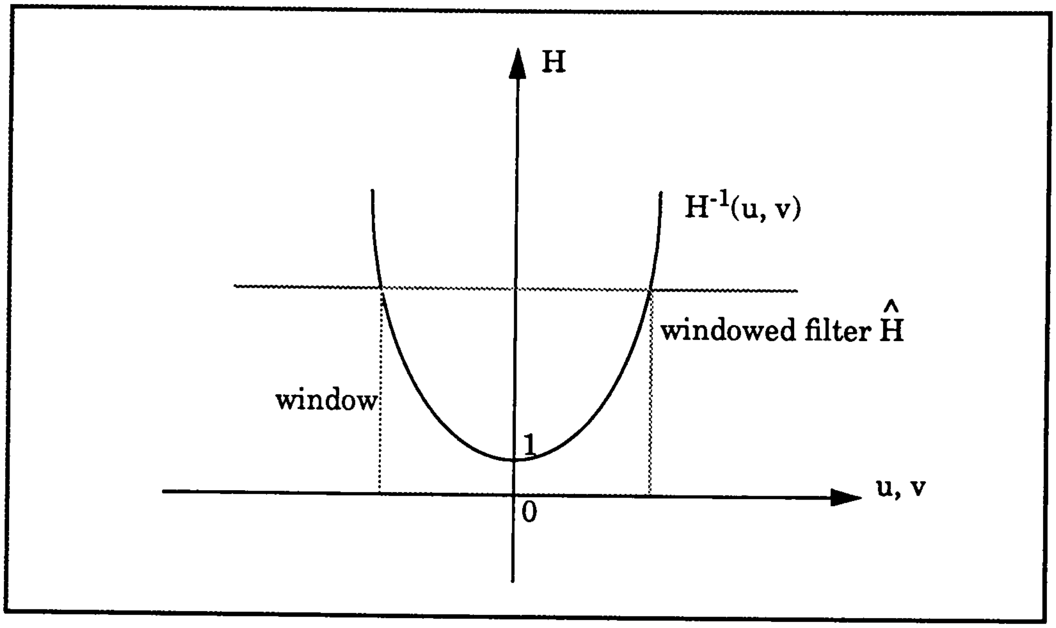

Figure 3.6 Profile of a windowed inverse filter

The "windowed" inverse filter as illustrated in Figure 3.6 is still a high-pass filter. Since noise represents a large portion of high frequency components, only the middle band is actually important. The very low frequency components contain information about the uniformity of the image and this information needs be preserved. Meanwhile, for simple and moderate control of the image quality, the filter is further modified into a band-pass filter as expressed in Equation (3.17) and illustrated in Figure 3.7.

$$\hat{H}(u,v) = \frac{A}{1+\left(\frac{u^2+v^2}{D_1^2}\right)^{k_1}} + \frac{B}{\left[1+\left(\frac{D_2^2}{u^2+v^2}\right)^{k_2}\right] \times \left[1+\left(\frac{u^2+v^2}{D_3^2}\right)^{k_3}\right]} \tag{3.17}$$

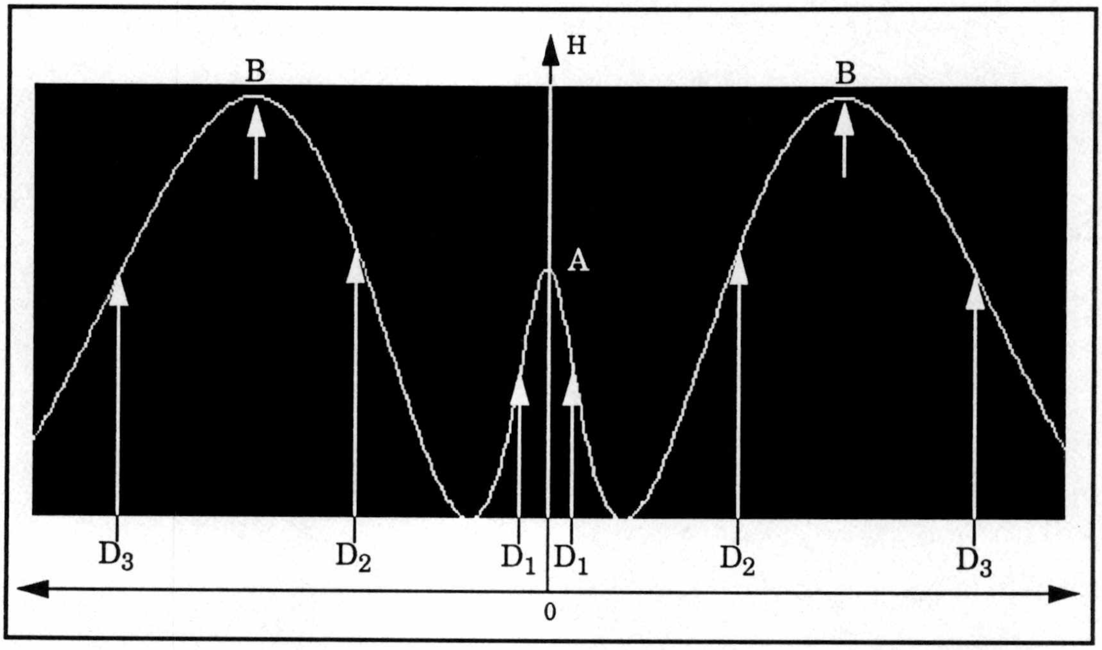

Figure 3.7 A One-Dimensional Profile of Modified Enhancement Filter

The filter is a combination of several Butterworth Filters [14]. There are two passing bands, one at very low frequency zone, including DC component, another is at the middle frequency zone. The first cut-off frequency is adopted from the direct inverse filter of Equation (3.16), the second cut-off frequency, is based on the estimation of random noise propagation.

The inclusion of the lower passing band helps to preserve the DC components and smooth the image. A drop-down at the higher-end of the filter reduces spurious noise in the new image while still highlighting the information of structural details. Figure 3.1c and Figure 3.1d (as well as Figure 3.1c and Figure 3.1d) display the results obtained by applying both a "windowed" filter as illustrated in Figure 3.6 and a modified filter (Equation (3.17)) respectively. Obviously, images filtered by a modified filter contains less noise. Figures 3.1d and 3.2d are the results of inverse filtering and Figure 3.8 is a 3-D surface plot of a image filtered by modified filter.

3.4 Image Enhancement II - Intensity Modification

3.4.1 The Problems and Solutions

As claimed at the beginning of this chapter, the intensity value of each individual pixel in the transmission image is not important for generating the sinogram since the μ value, attenuation coefficient, is assigned from a standard database. However, the pixel values can reflect anatomic structural information, while the procedure of inverse filtering has provided distinctive edge information. Intensity modification is used to correct the image intensity distribution to ease the segmentation procedure.

The image enhancement filtering reveals boundary information. However, filtering has also changed the image intensity distribution. There are two problems with the image's pixel values after filtering (see images of Figures 3.1d and 3.2d). First, some originally uniform areas are having higher intensity values. Second, extreme intensity changing appears around the objects' boundaries. These problems must be corrected, otherwise, image segmentation will yield incorrect results (see Figure 3.8, a surface plot of the image intensity Figure 4.2c).

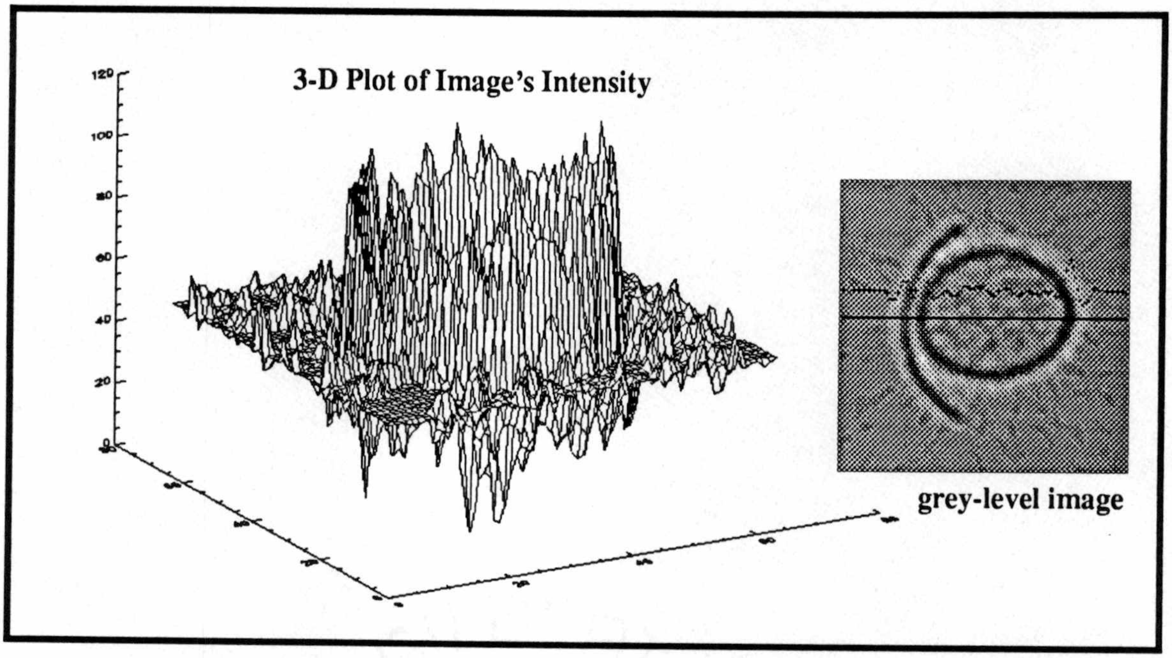

Figure 3.8 A 3-D Surface Plot of a Filtered Image

The causes of the above phenomena are obvious. The gray intensity in the uniform intensity areas are caused by rescaling of both the negative and the positive gradients of an image into a displayable, all-positive grey level. This elevates sandwiched zero-gradient solid areas onto a mid-ranged grey level. The frequency band-emphasized filter also causes wrinkles around the objects' boundaries and lowers the intensity of bright regions since any changes of an image are equally emphasized.

The intensity modification procedure invokes the original image as a criterion of correctness. There are two steps of modification, global modification and local correction. The global modification adjust the overall intensity distribution across the image, while the local correction corrects those pixels with extreme differences within their neighborhoods. Figure 3.9 shows the 3-D plot of the intensity of the images before and after applying the intensity modification techniques. Two other examples of using the compare-and-match scheme are also shown in Figures 4.1e and 4.2e, where the filtered images (Figures 4.1d and 4.2d) are enhanced with the image intensity well balanced and correctly mapped.

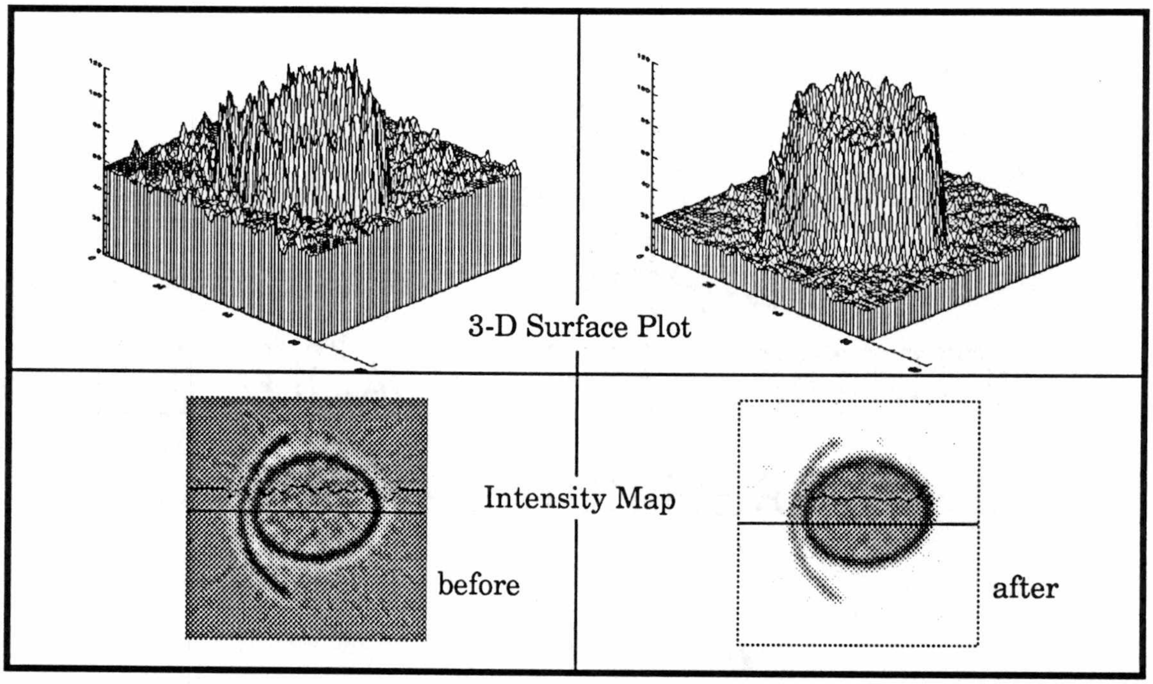

Figure 3.9 Images before and after Intensity Modification

3.4.2 Global Intensity Modification

Global intensity modification adjusts the general intensity distributions. Because the inverse filtering changed intensity distribution, global modification attempts to correct the intensity of each region to the value it was.

Filtered images are rescaled by assigning zero to the background. Weighted original image values are then added to them. The output is a calculated grey tone, and attenuation details yielding a clearer image. Equation (3.18) is the algorithm:

$$g(x,y) = [f(x,y) - bg] + w \times f_0(x,y), \tag{3.18}$$

where all-positive values $f(x,y)$, the result of the filter-process from the original image, are rescaled by background pixel value bg and the original image pixel value $f_0(x,y)$, weighted by weight factor w, is also added. The algorithm forces a zero-value at background, ensuring the correctness of the image's intensity distribution. Weight factor w is determined by balancing the noise removal effects and image detail clarity. An advanced scheme of implementation used in this project is to weight the original image value separately in the cases of positive and negative values of rescaled $f(x,y)$.

3.4.3 Local Intensity Correction

The global intensity modification merely corrects the problem caused by the changing of the magnitudes of each frequency components. Other problems like boundary effects and ragged intensity surfaces need be corrected by using local correction scheme.

The value of a pixel in the transmission image normally has relatively small variation among its neighbors. Assume at (x, y), $f(x, y)$ is the actual pixel value on the inverse-filtered image, $m(x, y)$ is the mean value and $\sigma(x, y)$ is the standard deviation within its neighborhood. $f_0(x, y)$ is the actual pixel value on the original transmission image, $m_0(x, y)$ is the mean value and $\sigma_0(x, y)$ is the standard deviation within its neighborhood. The corrected pixel value $g(x, y)$ is thus calculated by

$$g(x, y) = f(x, y) - [a \times d_m(x, y) + b \times d_\sigma(x, y)], \quad (3.19)$$

here,

$$d_m(x, y) = m(x, y) - m_0(x, y), \quad (3.20)$$

$$d_\sigma(x, y) = \sigma(x, y) - \sigma_0(x, y), \quad (3.21)$$

and a and b are the weight coefficient for $d_m(x, y)$ and $d_\sigma(x, y)$, respectively. The neighborhood shape can be rectangular or circular, and size may vary from 4 pixels to 32 pixels.

3.5 Image Segmentation

The segmentation procedure utilized here can be separated into two parts, thresholding and boundary detection. The thresholding is a feature clustering technique based on the image's gray-level histogram. Boundary detection, on the other hand, detects and link the boundaries according to the intensity gradient across the boundary points.

3.5.1 Regional Multi-Threshold Segmentation

The thresholding technique can be applied directly toward the original transmission images, since the intensity values of a transmission image correspond to the absorbance (or attenuation) of photons at that location. The enhanced image, however, provides better intensity information with less confusion and distortion among those regions with similar intensity. Therefore, multi-thresholding can be implemented for those regions with close intensity means in the original transmission image.

The criterion of the thresholding [14] starts with a two-segment image, the background and an object. The histogram of such an image may be considered as an estimation of the intensity probability function $p(x)$. This overall density function would be the sum or mixture of two unimodal densities, one for the object and one for the background. The mixture probability density function is given by,

$$p(x) = P_1 p_2(x) + P_2 p_2(x), \tag{3.22}$$

which, in case of Gaussian, is

$$p(x) = \frac{P_1}{\sqrt{2\pi}\sigma_1} exp\left[-\frac{(x-\mu_1)^2}{2\sigma_1^2}\right] + \frac{P_2}{\sqrt{2\pi}\sigma_2} exp\left[-\frac{(x-\mu_2)^2}{2\sigma_2^2}\right], \tag{3.23}$$

where μ_1 and μ_2 are the mean values of the two intensity models, σ_1 and σ_2 are their standard deviation about the means, P_1 and P_2 are the probabilities of the *a priori* models, and satisfy constraint

$$P_1 + P_2 = 1. \tag{3.24}$$

Therefore, an optimal threshold (in terms of minimum error) T can be easily calculated by a quadratic equation

$$AT^2 + BT + C = 0, \tag{3.25}$$

where,

$$\begin{aligned} A &= \sigma_1^2 - \sigma_2^2 \\ B &= 2(\mu_1\sigma_2^2 - \mu_2\sigma_1^2) \\ C &= \sigma_1^2\mu_2^2 - \sigma_2^2\mu_1^2 + 2\sigma_1^2\sigma_2^2 ln\left(\frac{\sigma_2 P_1}{\sigma_1 P_2}\right) \end{aligned} \tag{3.26}$$

Although transmission images contain more than one object, the image can be simplified by applying the multi-thresholding method. The windowed multi-thresholding scheme is a collection of several single-thresholding procedure. In a brain study, for example, the first step separates the background and brain region, the second thresholding then takes place within the brain region to separate skull of brain from other soft tissue, such as grey matter. Sometimes, the sinus area is separated at the first step, since it is filled with air and the attenuation coefficient is closer to that of background than the average attenuation value of brain. The depth of such thresholding can either set by the operator interactively or based on the criterion of thresholding. The latter method tests whether T_n is close enough to one of the two mean values, μ_1 or μ_2. If so, the procedure is terminated, thus producing only *n-1* threshold values and clustering *n* different types of segments.

3.5.2 Boundary Detection, Edge Sorting and Noise Removal

Because the image has already be segmented by multi-thresholding, boundary detection is thus as easy as finding the edge between black and white. The operator is

$$G[f(x,y)] \cong |f(x,y) - f(x+1,y)| + |f(x,y) - f(x,y+1)|. \tag{3.27}$$

Here, if $G[f(x,y)] > 1$, an edge point is found [15] [16].

Usually the edge detected through the above scheme is a closed contour. Different edge segments must be sorted for further use in interactive redrawing and attenuation coefficient assignment. Also after sorting, some small region which have high probability to be noise are removed.

The scheme developed for this procedure is an edge sorting and noise removal process. The scheme searches along each region's boundary, defined by the boundary detection procedure. Any breaking points will be found and linked. Each piece of closed boundary is sorted. The area of each region and the length of boundary are calculated. If both the area and length are smaller than given thresholds, this region will be removed.

The output after the whole procedure is a boundary image. Those boundaries scratch out the shapes of all the attenuation matter within the cross-section of the transaxial transmission image. The corresponding attenuation coefficients are filled in from the attenuation coefficient table, and the ACF sinogram is calculated using a forward projection algorithm.

CHAPTER 4. EVALUATION

The evaluation of the Adaptive Attenuation Correction Tool consists of two parts, the phantom studies and clinical patient emission PET image studies. The purposes of this chapter is to evaluate:

The ability to enhance transmission scan,
The optimal scan time for short transmission scans,
The visual and statistical results of attenuation corrected emission data.

The evaluation procedure and statistical data are shown in the following.

4.1 Phantom Studies - Transmission Images

A set of phantom studies were conducted. The phantom is a plastic barrel filled with water. Transmission scans were taken in the mid-transaxial plane, with scan times varied from 1 minutes to 100 minutes. The original transmission images of those scans are shown in Figure 4.1 and Figure 4.2. Table 4.1 shows scan time vs. total counts in each image.

Table 4.1: Scan Time (minutes) vs. Total Counts

s.t.	1 min.	2 min.	3 min.	5 min.	10 min.	15 min.	20 min.	100 min
cnt.	335.4 K	670.4 K	1.005 M	1.674 M	3.353 M	5.027 M	6.700 M	33.51 M

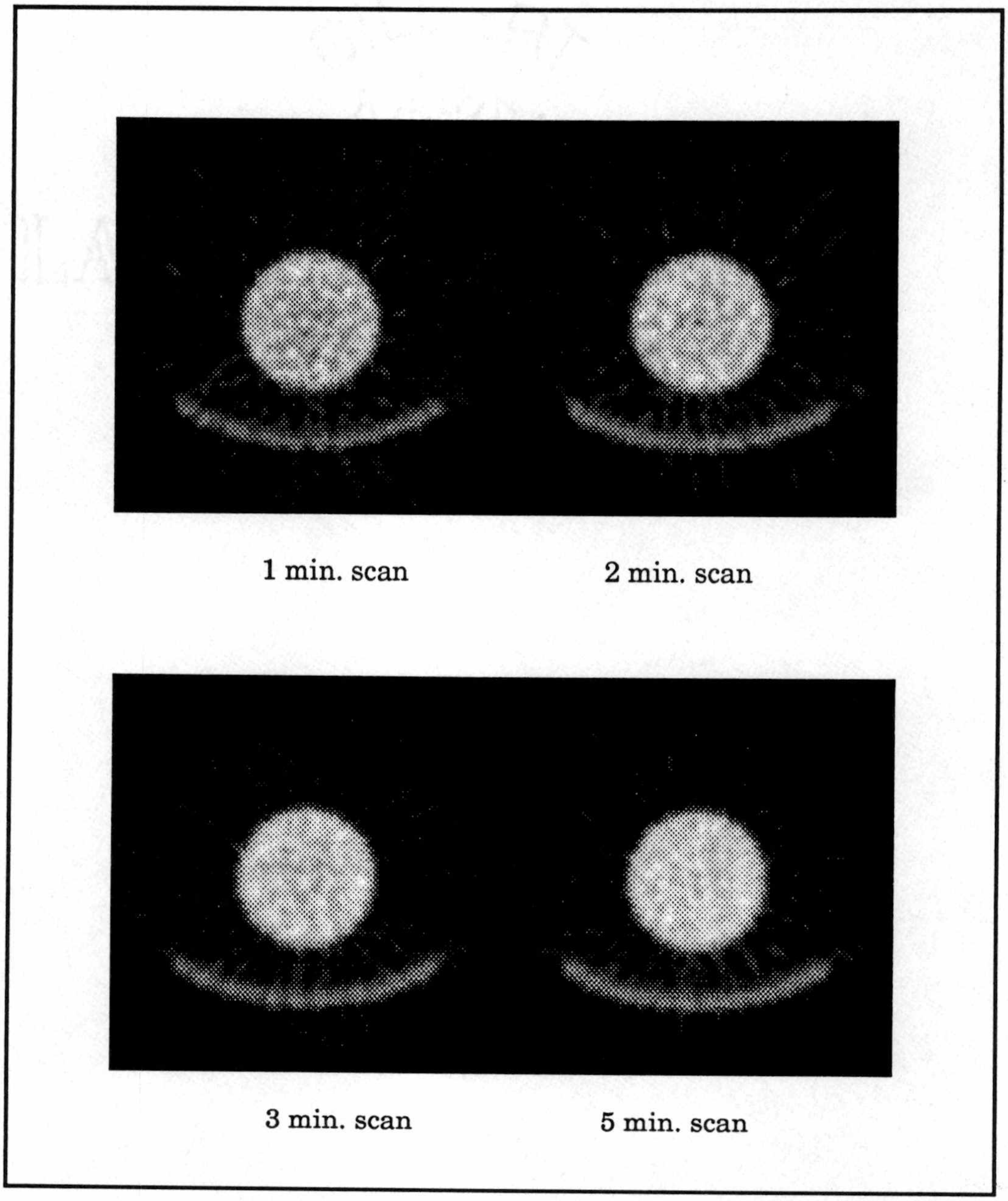

Figure 4.1 Uniform Cylinder Phantom Transmission Scan Images (Part I)

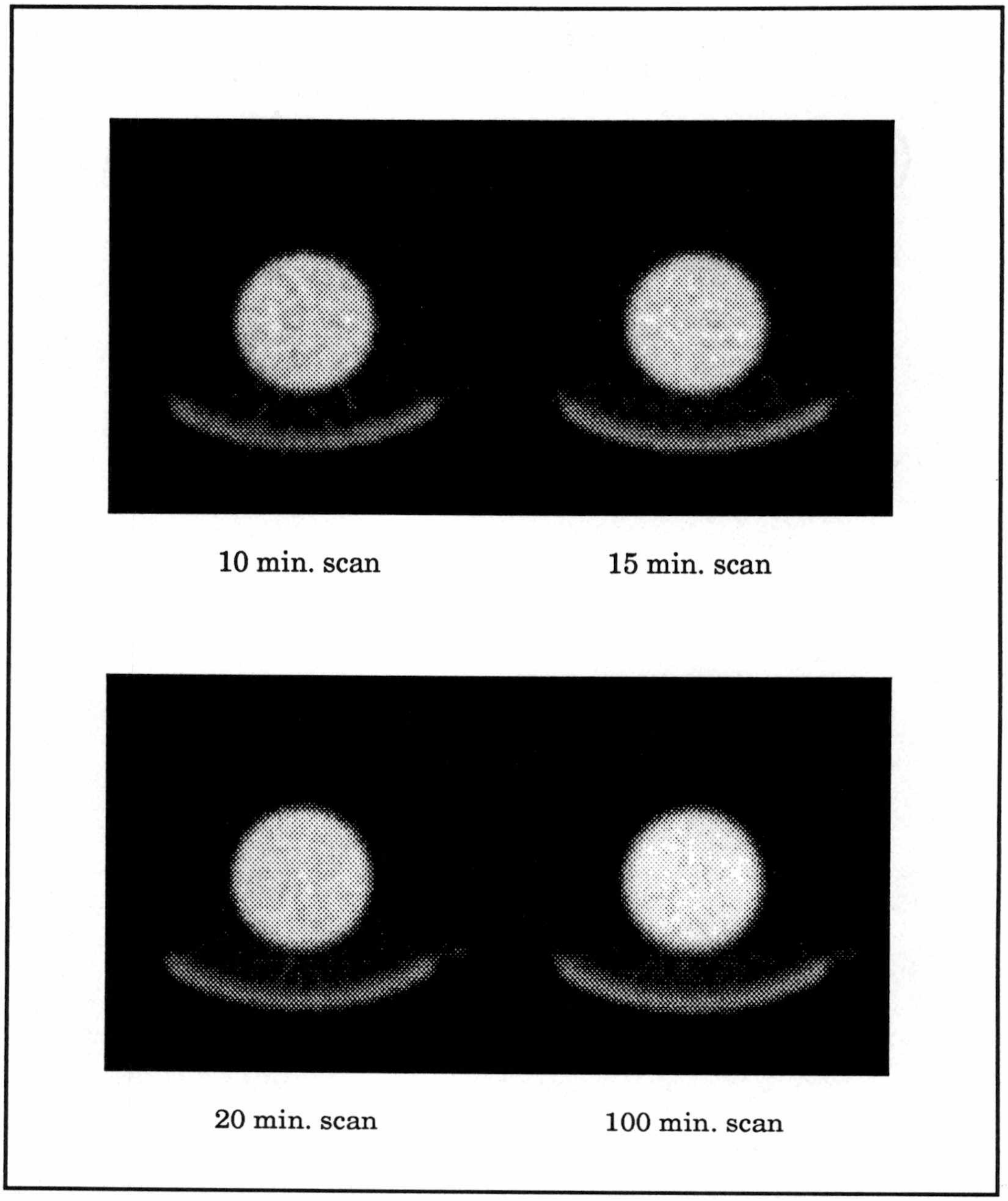

Figure 4.2 Uniform Cylinder Phantom Transmission Scan Images (Part II)

The cross-section image of the phantom consists of only four regions, the background, the holder, the water, and the wall of cylinder. Several studies were conducted to evaluate the quality of image processing procedures developed in this project.

4.1.1 Study I - Uniformity Preservation vs. Boundary Distinguishability

The purpose of this study was to examine the enhancement process's ability to distinguish the edges of structures while reducing noise within the structures. This study also attempts to determine the optimal scan time (which must be less than a conventional 20 minutes scan) for use with image processing procedures. The measurements were taken by the Imagetool, which calculated the mean and standard deviation of selected region-of-interest (ROI).

The first two sets of measurements listed in Table 4.2 and Table 4.3 were taken from two types of transmission images, the original transmission images and those processed transmission images. Both tables show the mean, standard deviation and coefficient of variance of two major regions, the water and the background. These two sets of data reveal how the image processing procedures can preserve the uniformity of those regions while still distinguishing the boundary information. Here the standard deviation is expected to be low, although the processed images show mild increase in overall noise as manifest by an increased coefficient of variance.

The third set of measurement listed in Table 4.4 were taken from a narrow ring-shaped ROI which barely covers the boundary region between the wall of the cylinder and air. Here, the standard deviation roughly shows the edge noise generated in the processing procedures.

Table 4.2: Noise Analysis on Phantom Transmission Studies (Original)

scan time (mins.)	background			object		
	mean	s.d.	s.d./mean	mean	s.d.	s.d./mean
1	0.000	0.003	N / A	0.083	0.008	9.6 %
2	0.000	0.003		0.088	0.006	6.8 %
3	0.000	0.003		0.090	0.006	6.6 %
5	0.000	0.002		0.091	0.004	4.4 %
10	0.000	0.002		0.092	0.003	3.3 %
15	0.000	0.001		0.092	0.003	3.3 %
20	0.000	0.001		0.093	0.003	3.2 %
100	0.000	0.000		0.093	0.002	2.2 %

Table 4.3: Noise Analysis on Phantom Transmission Studies (Processed)

scan time (mins.)	background			object		
	mean	s.d.	s.d./mean	mean	s.d.	s.d./mean
1	0.000	0.004	N / A	0.083	0.012	14.5 %
2	0.000	0.004		0.082	0.010	12.2 %
3	0.000	0.004		0.090	0.008	8.89 %
5	0.000	0.004		0.091	0.007	7.69 %
10	0.000	0.003		0.092	0.005	5.43 %
15	0.000	0.002		0.092	0.004	4.35 %
20	0.000	0.002		0.093	0.004	4.30 %
100	0.000	0.000		0.093	0.003	3.23 %

Table 4.4: Boundary Distinguishability on Phantom Study

scan time (mins.)	from original image (mm)			from enhanced image (mm)		
	mean	s.d.	s.d./mean	mean	s.d.	s.d./mean
1	0.041	0.027	65.9 %	0.043	0.028	65.1 %
2	0.042	0.027	64.3 %	0.044	0.028	63.6 %
3	0.042	0.026	61.9 %	0.043	0.028	65.1 %
5	0.043	0.026	60.5 %	0.044	0.027	61.4 %
10	0.043	0.025	58.1 %	0.044	0.027	61.4 %
15	0.044	0.025	56.8 %	0.045	0.027	60.0 %
20	0.044	0.025	56.8 %	0.045	0.027	60.0 %
100	0.045	0.026	57.8 %	0.045	0.028	62.2 %

Standard deviation is not a perfect indicator. The standard deviation of an ROI across the boundary region reflects a combination of edge noise level and edge gradient. However, the edge gradient effect increases slower than the scan duration time increases, and the edge gradient effect can be constant for each image (except 100 minute scan) within the ring-shaped ROI; therefore changes in standard deviation are considered to be due to edge noise. The results show an acceptable noise level for a processed 5 minute transmission scan. This noise level (61.4%) is similar to that of longer duration scans (60.0 - 62.2% c.v.).

4.1.2 Study II - Geometrical Information Study

This study attempts to evaluate the quantitative results using the image processing procedure on the transmission scan image. The geometric information about the attenuation structure is very important for the correctness of emission data, therefore, the distortion of the geometric information must be reduced, at least not increased, after the enhancement procedures. This is extremely difficult with a procedure involving high frequency processing.

The diameter of the outside wall of the cylinder is 200.00 ± 0.5 mm using 8 measurement from 8 different angles at 45° intervals (Measure tool: SQUIBB stainless steel ruler, with minimum measurement unit 0.5 mm).

The diameter measured from the image was actually the pixel number times the resolution per pixel. The images were first thresholded into a binary image, then the object diameter was drawn and measured using *Imagetool* developed by CTI for ECAT 931 PET system [26].

Table 4.5: Diameter Measurement of Phantom before/after enhancement

scan time (mins.)	from original image (mm)			from enhanced image (mm)		
	mean	s.d.	s.d./mean	mean	s.d.	s.d./mean
1	196.9	6.56	3.34 %	194.2	8.26	4.25 %
2	195.6	5.46	2.79 %	194.5	7.83	4.03 %
3	198.3	5.10	2.57 %	195.7	6.22	3.18 %
5	198.2	4.24	2.14 %	197.3	4.33	2.19 %
10	199.1	3.25	1.63 %	198.8	3.42	1.72 %
15	199.6	3.06	1.53 %	199.4	2.53	1.27 %
20	200.2	3.02	1.51 %	200.1	2.14	1.07 %
100	199.9	1.52	0.76 %	200.1	1.32	0.66 %

As Noted in Table 4.5, due to the broken linkage of those images with very short scan time, i.e., 1 or 2 minutes, the measurements were relatively rough and inaccurate, which is shown by their standard deviations. There is no reduction in geometric image quality identified as a result of the enhancement process at times greater than 5 minutes (2.19% c.v of enhanced image vs. 2.14% c.v of original image).

The above two studies from transmission images show that the image processing procedures adopted in the Adaptive Attenuation Correction Tool perform more successfully on edges than inside uniform matter because of the high frequency effect. It is feasible to process a scan as short as 5 minutes while still yielding better edge information with a slight trade-off in noise level.

4.2 Phantom Study - Attenuation Correction on Emission Data

This experiment is to measure the effectiveness of using the Adaptive Attenuation Correction Tool. Here a phantom with low activity of emission is used. Again it is a uniformed cylinder filled with low concentration of Ga-68. Three sets of images were taken: a 20 minutes emission scan and two transmission scan, one is 5 minutes and another is 20 minutes.

The emission data was reconstructed with four types of attenuation correction sinograms, (1) 5 minute transmission sinogram, (2) 20 minute transmission sinogram, (3) processed sinogram using 5 minute transmission image, and (4) processed sinogram using 20 minute transmission image.

Table 4.6 is a list of measurement within two typical ROIs, the background and the object for each of the four emission images.

Table 4.6: Emission Phantom Image Quality Analysis

Image ID	background			object		
	mean	s.d.	s.d./mean	mean	s.d.	s.d./mean
1	0.000	0.009	N / A	0.081	0.021	25.9 %
2	0.000	0.008		0.082	0.013	15.9 %
3	0.000	0.008		0.081	0.013	16.0 %
4	0.000	0.007		0.082	0.011	13.4 %

Figure 4.3 show all four images with the same order. Notice there is little visual difference among images 2, 3, and 4, especially images 3 and 4. This is because the attenuation maps of the last two are almost identical.

The conclusion from this study is that for simple objects, a 5 minute transmission scan is sufficient for the Attenuation Correction Tool to generate a good attenuation sinogram. Also as noted, the result of the Adaptive Attenuation Correction Tool generates a uniformed attenuation coefficient map for each attenuation system; therefore, as long as the accuracy of the edge information is guaranteed, longer duration transmission scans would not result in improvements.

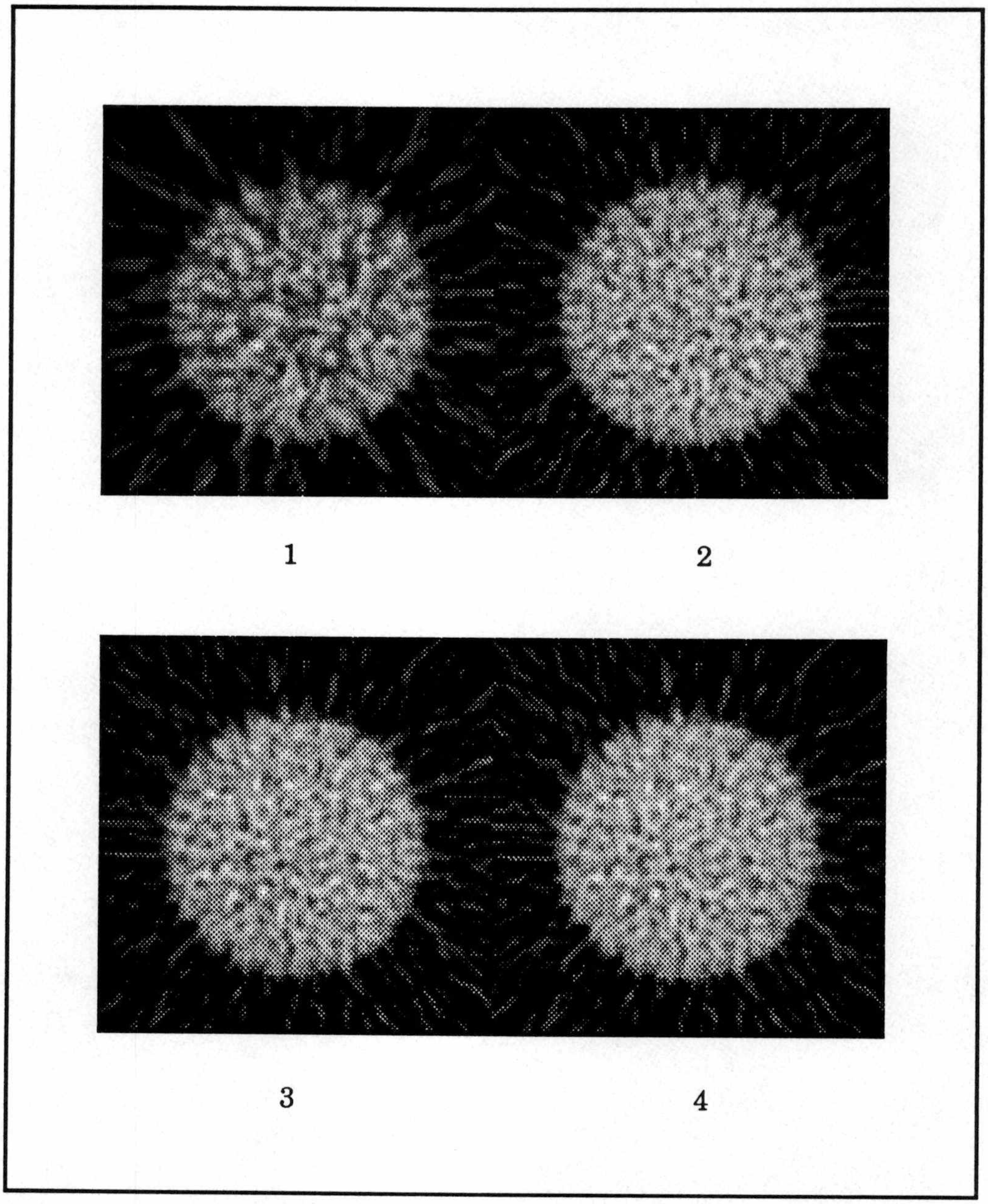

Figure 4.3 Emission Images with different Attenuation Correction Sinograms

Image ID numbers are corespondent to the description in the second paragraph of Section 4.2 and Table 4.6.

4.3 Attenuation Correction Tool on Clinical PET Applications

Clinical images were reconstructed with the Adaptive Attenuation Correction Tool and the conventional measured attenuation correction method.

Figure 4.4a is a set of uncorrected emission images. Using The Adaptive Attenuation Correction Tool, the attenuation structures were drawn on the information provided from uncorrected emission data (i.e. Figure 4.4a), and attenuation correction sinograms were created. The new emission images (Figure 4.4b) were reconstructed using these attenuation correction factor sinograms. The whole procedure on the Adaptive Attenuation Correction Tool with 15-plane images set took approximately 30 minutes, plus additional 20 seconds per plane of reconstruction time (unattended).

Note that internal structures not visible in image set 4.4a can be seen with attenuation correction in images set 4.4b. This demonstrates the potential of the Adaptive Attenuation Correction Tool to provide improved visual image information. Furthermore, accurate shapes of attenuation structures with the Adaptive Attenuation Correction Tool can possibly provide finer quantitative measurements and higher signal-to-noise ratio.

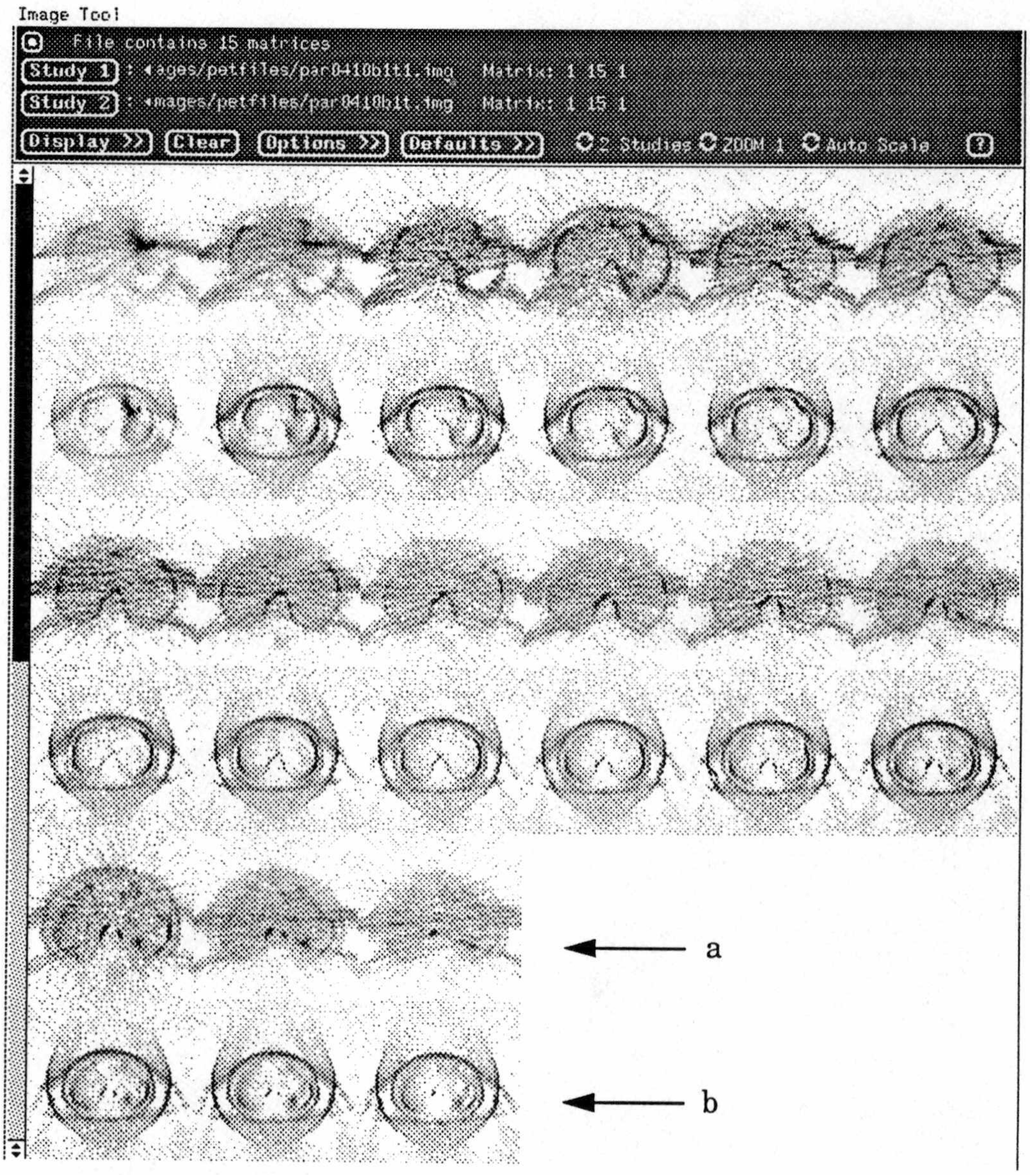

Figure 4.4 Emission Images after (a) and before (b) attenuation correction using AACT

CHAPTER 5. SOFTWARE DEVELOPMENT

This chapter will introduce some of the important techniques which emerged during the developing of the Adaptive Attenuation Correction Tool (AACT) software. This is necessary because programming was an important part of the implementation of the algorithms. This chapter will address some practical tips gained from experience while working on the project.

The next several sections will introduce the SunView Window System [17], which provides a strong, multifunctional and friendly graphic user interface (GUI), the SunView's application in this package, the flow charts of the software, some typical data structures adopted, the use of remote procedure calls (RPC) [18], and the matching between this package and other image tools for ECAT PET systems developed by CTI (Siemens/CTI, Inc. Knoxville, Tennessee) [19].

5.1 Window System Programming Environment

The "Adaptive Attenuation Correction Tool (AACT)" is developed and runs completely under the SunWindow system [20-22]. SunView (Sun Visual/Integrated Environment for Workstations) is a programming environment providing a user-interface toolkit to support interactive, graphics-based applications which runs within

SunView windows. It consists of two major areas of functionality: building blocks for output and a run-time system for managing input. Thus, it is a suitable environment for an object-oriented package like the Adaptive Attenuation Correction Tool. It has the advantage of supporting relatively independent running executables which communicate with other procedures. That means, if used as stand-alone, it is an independent tool; but it can also cooperate with other software to form a complete tool-package.

5.1.1 The SunView Graphic User Interface

SunView is an object-oriented programming environment for Sun Workstation's unique window system, SunWindow. A typical SunView application includes three parts: objects, windows and notifiers. An object is a visual building block which is used to assemble the user interface to the application. A window is a kind of object, but it acts as a functional interface. The implementation of the object is not exposed; the manipulation of an object is performed by passing its unique identifier, or "event", to its associated function. This "event-driven" style is the basic character of programming in this tool.

In this tool, the building blocks include panels containing *buttons*, *choice items*, *pull-out menus*, *analog sliders*, and *canvases* to control the system input, process output, and display the results of system's process. The run-time system which manages the input is a set of those functions which handle and process the images, i.e. loading images, enhancing images, segmenting images, attenuation factor mapping, and saving the attenuation correction sinogram. All these functions are driven by building blocks, such as buttons, choices items and menus, which the user can see during the program execution. Hidden from the user, "notifiers" actually drive the process forward. In the subsequent section, the author will discuss some of the important methods implementing the window system for this tool.

5.1.2 The Objects

The objects are the collection of all the visual building blocks. A *window* is its major subset and is discussed separately. *Menu, icon, pointer, panel item, scrollbar* and *alert* are all objects. In the Attenuation Correction Tool, *menu, icon, pointer* and *panel items* are used frequently.

5.1.2.1 Window objects

Window objects include *frames* and *subwindows*. A *frame* is not useful itself. It *owns* the *subwindows* and the *frames* it contains. Thus, the whole window system forms a hierarchical structure. The *base frame* is at the top of this hierarchy for each system. Logically, only the *base frame* can be *iconified.* Notice that an application is not necessarily limited to having only one *base frame*.

Frames contain non-overlapping *subwindows* within their borders. There are four types of subwindows provided by SunView. Those types are *Panel Subwindows, Text Subwindows, Canvas Subwindows* and *TTY Subwindows*. In the Attenuation Correction Tool, only the *panel* and the *canvas* are used.

Panel is a subwindow containing panel items (see section 6.1.2.2), so it is a subwindow conducting management and controlling the system. In the Attenuation

Correction Tool, most of the handling and control are processed through items on the panels. The panel window turns out to be a control desk. The user can find examples in the next chapter.

Canvas is the subwindow on which programs can draw. It is like a graphic terminal or image displayer. In this project, the program performs three major tasks on canvas: displaying images, overlaying graphics, and filling regions. The SunView's canvas accepts only raster formatted image data and stores in the system's kernel for faster render and display [20]. Graphics overlay and regions fill work on a pop-up window's canvas. For a gray level image display, SunView uses a specified color table, which is set and altered by a separate procedure called "colortool" (CTI, Inc., Knoxville, Tennessee) through RPC (Remote Procedure Call). The color table is discussed in Section 6.1.4.

5.1.2.2 Other visual objects

Other types of objects, like windows, are displayed on the screen, but are less general and more tailored to their specific function. The functionality of panel items, menus, the pointer and the icons in relation to the Attenuation Correction Tool will be discussed later.

A panel item is a component of the panel that facilitates a particular type of interaction between the user and the application. Panel items can be moved, displayed and undisplayed through program control. For example, in the tool, when the user presses the "AutoProc" button on the main panel, the "DispImag" and "SinoGram" buttons vanish and are replaced by the choice items for image enhancement and the "GO" and "Cancel" buttons for actions. When the enhancing process is finished, those panel items disappear and the main panel items reappear. There are several predefined types of items with predesigned patterns, including *buttons, message items, choice items, text items*, and *sliders*. For needed specialization, programmers can also design their own customized panel items performing specially designed functions.

Menus are another kind of object which carry out tasks similar to what panel items do. The user can find the menus throughout the Attenuation Correction Tool. They mainly exist on the canvas, but some buttons have menus, as well as some of the choice items, which work as a cycle. Menus provide not only the choices, but also the ability to control the programs. Menus are normally activated by the mouse's right button.

A pointer is the object indicating the mouse location on the screen. It is the most basic object to accomplish any interaction within the window environment. The icon, on the other hand, is just a logo representing the application when its window is closed.

5.1.3 The Notifiers

All objects are actually interfaces between user interaction and program control. When panel items are "clicked" with the mouse's left button, the procedures which are controlled by panel items are activated to carry out the requested process (see Figure 5.1 on page 64). These kinds of procedures are the "Notifiers". From the

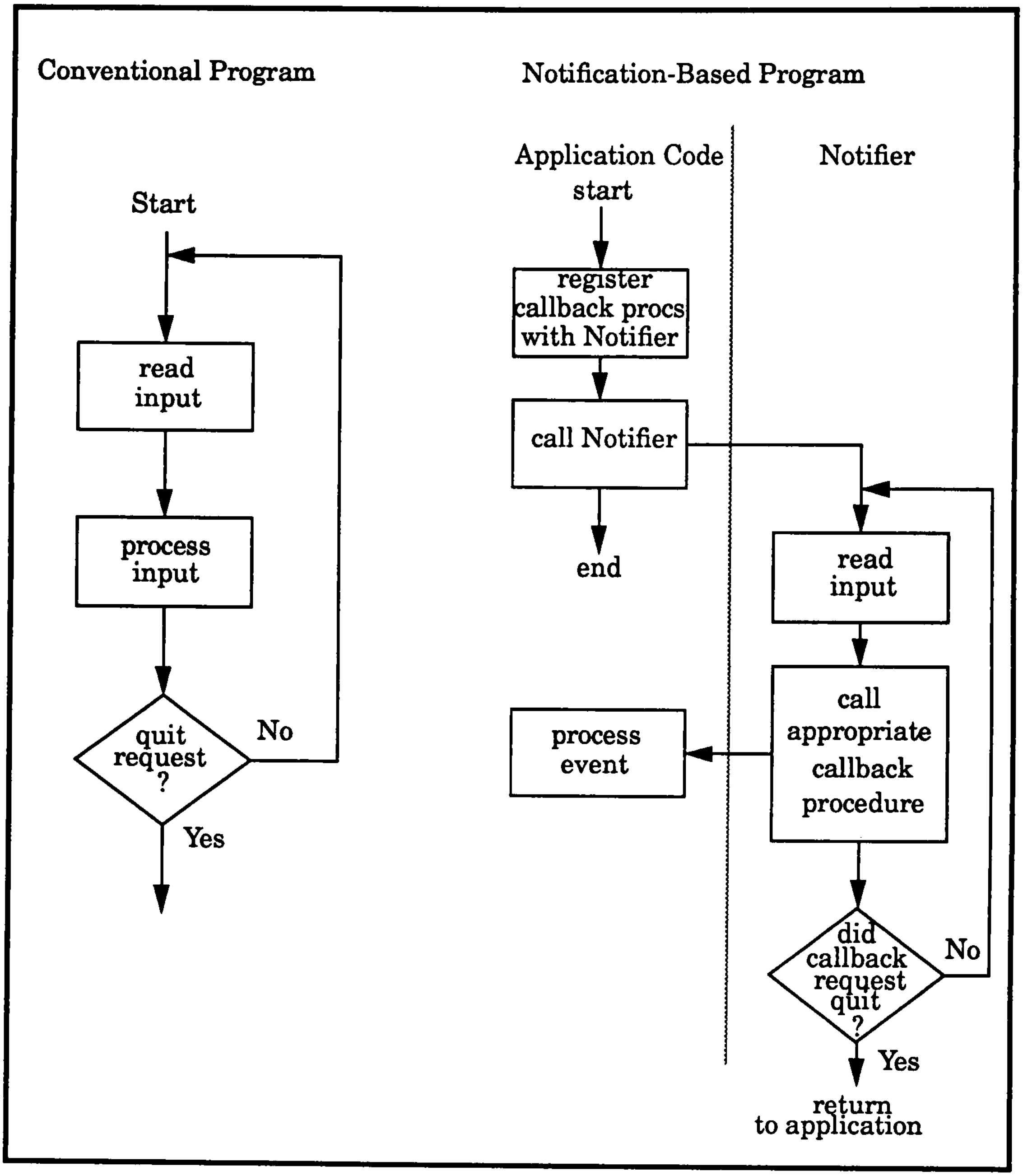

Figure 5.1 Control Structures of Two types of system.

Notification-based system (right) inverts the "straight line" control structure (left). The main control loop resides in the Notifier rather than the application. These procedures are called "notify procs" or "callback procs".

view of the system, the notifiers are the input which control and directs the flow of operation.

SunView is a *notification-based* system. The *notifier* acts as the controlling entity within a user process, reading UNIX input from the kernel, and formatting it into higher-level *events*, which distributes to the different SunView objects. One big advantage of the notification-based system is that it centralizes all the components of the application. By simply passing the event needed, the user can directly control each component, which releases the burden of managing a complex, event-driven environment from the non-centralized, straight line flow of control. In this tool, all the notifiers are directed by the panel items and menus through events, so that it enables the user to interact with the *notifiers* directly. The *menus* on canvas are controlled by the canvas events handler.

5.1.4 Color Table

The *color table* for programming the SunView applications is another important factor. In SunView, all the *frames, subwindows, panel items*, and *menus* can be applied with different colors through color table. This is mostly ignored by SunView programmers, due to the lack of detail in the SunView Programmer Guide [20]. Nevertheless, in preparing this tool, several approaches were tried, and some results were applied to the tool as described below.

The color for objects is merely for the purpose of visual improvement and comfort of the eyes. However, the color table on canvas is very important for displaying grey level images. The Sun Window System is able to display millions of different colors on its screen, but only 256 different colors can be displayed on the screen simultaneously. That facts means the system needs only 8 bits for displaying the colors on the screen. That is also the reason the color table is so important to SunView. The color table has 256 segments, each segment represents a predefined color, which is a combination of red, green, and blue, each ranges from 0 to 255 (8 bits each). The process of setting up such a color table is called "mapping" the color, and the color-table is usually referred as *cms*, color map segments. On the canvas, the grey level image can be displayed with its grey intensity mapped to the appropriate colors. That is what the "colortool" (CTI, Inc., Knoxville, Tennessee) does, with different color tables giving different color maps such as rainbow, hot metal, bronson, and many more. Among the 256 colors, the system has already set 0 to the background colors of the screen and 1 to the foreground color. The system uses color segments numbered for 128 - 255. Thus, the only available color segments for displaying the canvas grey level image are those indexed from 2 to 127. Normally, the segments from 120 to 127 are set to the fixed colors of black, white, grey, pink, yellow, red, green and blue, for graphic overlay, leaving only 2 to 119 for grey level displaying. In other words, the intensity of each image must be rescaled to the range between 2 and 119 before it can de displayed on the tool's canvas.

5.2 General Flow of Control

The Adaptive Attenuation Correction Tool is a multi-step processing package. Its complete details of operation can be found in Chapter 7 which expresses them from the user's point. In the rest part of this section, the flow of control in the Attenuation Correction Tool processors will be illustrated by flow charts along with explanation.

5.2.1 Conventional Programming Flow Charts

Conventional programming methodology arranges process blocks according to the order of processing. Each process is executed successively by a preset order. The branches can be controlled through the user's interaction, similar to syntactic *questions and answers* control. A general flow chart of a single image processing can be segregated into several major parts as illustrated in Figure 5.2. If we consider the Adaptive Attenuation Correction Tool as a black box, then this box has actually one main entrance and one main exit. The entrance takes the input, which must be the standard PET transmission images file. The output from the exit will be the standard PET attenuation correction sinogram file. This attenuation file will be used later for the reconstruction of the PET emission scan. Since this tool is not exactly a black box, and the user is required to review and accept most of the intermediate result during the process, dialogue interfaces appear during execution of the process allowing user's control during the real time processing. Because each file contains more than one image (normally 15 images or 31 images depending on the model of PET Scanner), there must be a loop between the blocks of "display" and "sinogram". The tool will not

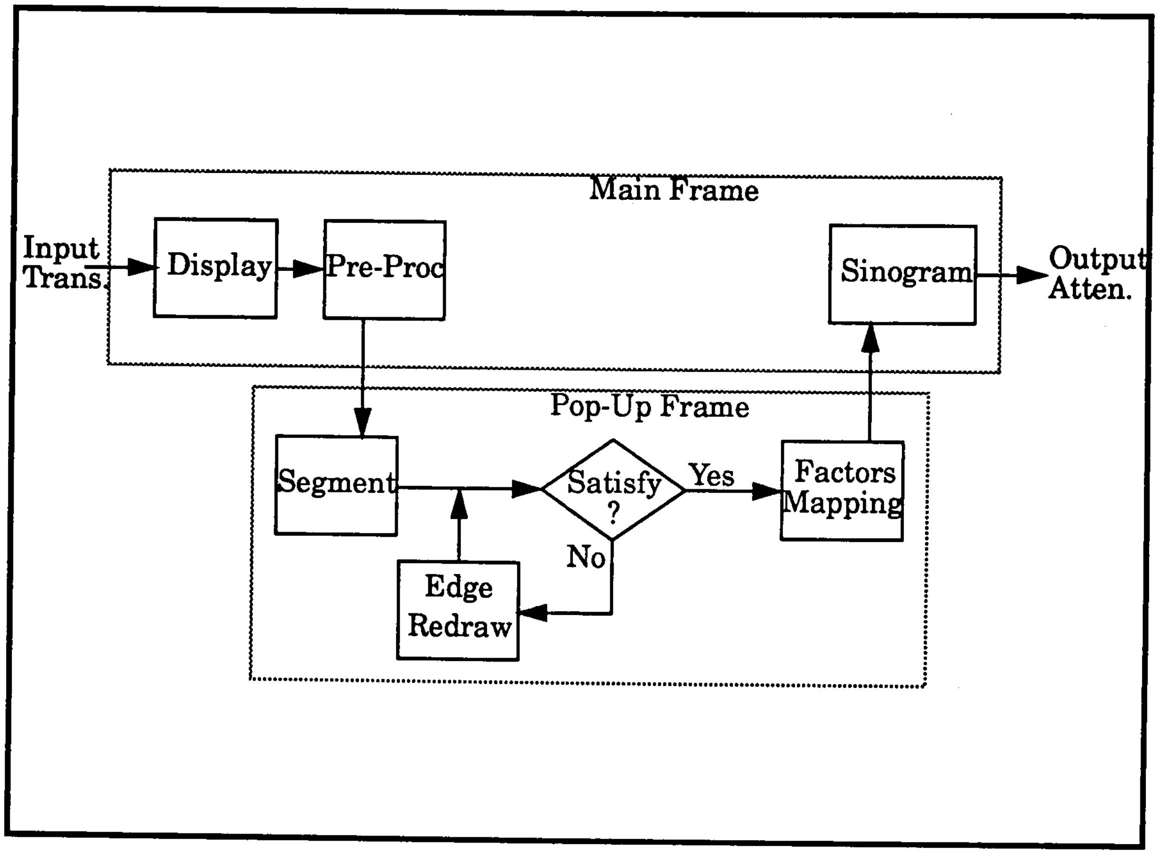

Figure 5.2 General flow of control of AACT.

calculate the sinograms or save them on the disk until all the images in the file are processed.

There are three functional blocks in main canvas. “Display” is a general-function block. When an image file is loaded, the entire set of images must be displayed before performing any further processing. The “display” function is also built for displaying other types of images in the system memory which are generated as intermediate results during the process. “Pre-Proc” is the block that does image enhancing. At the beginning, the program will let the user choose the filter type and set the parameters for smoothness. Both blocks can handle either a single image or all the images of the file. “Sinogram” is the last block of the main canvas. It performs the complete forward-projection from each attenuation map and calculates the exponential of the summation of each projection beam. The result is saved on the disk in standard PET attenuation file format. After finishing, the control either returns to the beginning of the flow or terminates the process.

The pop-up window consists of three blocks. “Segment” is similar to “Pre-Proc” in the main frame, it allows the user to set filter parameters and detects the edge of each anatomic region. “Edge Redraw” is a complement or alternate block which functions to correct the boundaries generated from “Segment”. “Factors Mapping” is the last stop in the flow within the pop-up frame. After the attenuation factors are assigned to their appropriate regions, the pop-frame is killed. The attenuation factors map will be displayed on the main canvas and the data will be saved in the system memory.

5.2.2 Notification-Based Programming Structure

As noted in the last section and Figure 5.2, each block performs its designated role at certain stages of the entire process. However, it is not necessary to say that each block can only perform at certain points and the that these blocks have to take an action in a certain order. For example, "Display" is a function that can take place at any stage of the process and can display the three different types of images upon the users' request and the images' availability. "Edge Redraw" does not have to be performed after "Segment", since the user can make the decision to reject or accept the segmented image. On the other hand, some blocks must operate after other blocks finish. For example, "Sinogram" must always be the last stop of the entire flow. Thus, different blocks are designed for different purposes and with different priorities. Handling such flexibility in conventional programming can be difficult. Figure 5.3 illustrates the actual control among objects in the Adaptive Attenuation Correction Tool.

During the actual programming, each object is built separately with its own notifier. Each notification control includes four parts: starting, stopping, mass destruction, and scheduling. In starting, if the user issues a wrong control event, the tool's notify procedure will check if it can execute the command and give the appropriate feedback. For example, if the user tries to execute the "sinogram" right after loading the images, the program will reject the command and generate an error message. Stopping means a normal termination of the notify procedure. During the implementation of the Attenuation Correction Tool, some of the notify procedures are computational intensive and are very time consuming, like "Pre-Proc" and "Sinogram", so it is

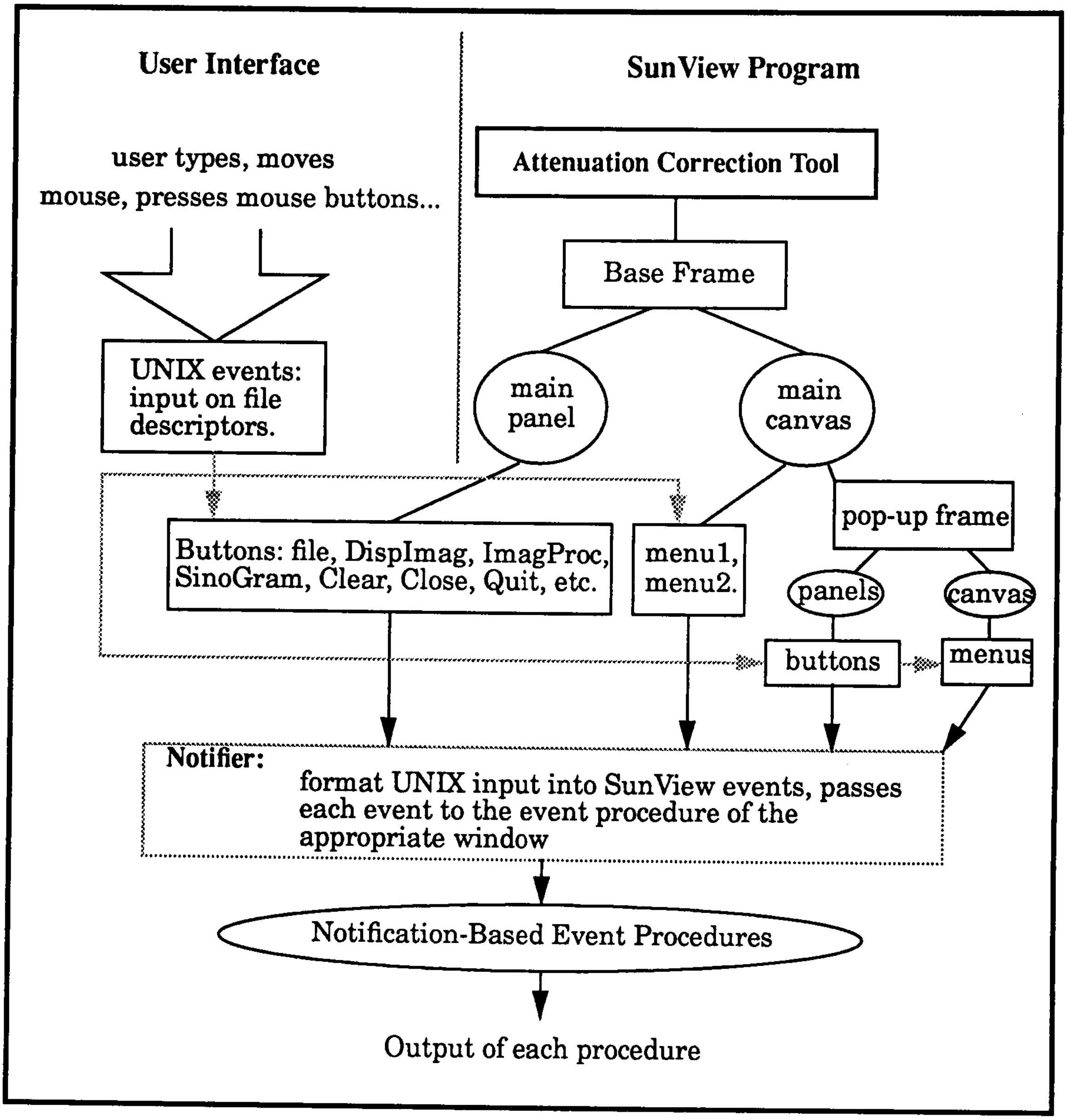

Figure 5.3 Structure of the AACT

necessary to segregate the notify procedure into several small pieces in order to include a notify-time-out function. This allows the users to interrupt the procedure by calling time-out without destroying the flow of control. For example, the "STOP" button enables termination of the process while displaying, enhancing, or calculating the sinogram of an entire set of images. Scheduling arranges the notify procedures to run in order. Mass destruction, on the other hand, will destroy all the running procedures unconditionally, like using "Control-C" from the keyboard. This type of structure allows the user easy access and easy control of executing functions.

The notification-based programming not only orders the notifiers, but also centralizes all the functional blocks into an event-driven environment. Each application receives only the events the user has directed towards it. In Figure 5.3, the program can be divided into three levels. Regardless of the flow of control, these three levels are (1) the user interface, which includes user's input from the keyboard and mouse. (2) SunView events, and (3) notification procedures. The user provides control through the user interface, which is converted into SunView events and passed to the respective notify procedure. Thus, the straight line flow of control is replaced by user's control to prevent the process from going in the wrong direction. Although it is not straightforward to program, it is very user friendly, especially for software that requires a lot of user interaction.

5.3 Using of Data Structure

Because the Attenuation Correction Tool handles both the input images and the interval results as well as a variety of graphics, using the data structure wisely and efficiently is another important issue. This package is written in the C Programming Language (Sun C), in coalition with SunView's object-oriented window system programming package. The approach gains all the advantages of both languages' data structure options. The data structure built in this package can be sorted into two major categories: programming data types and system provided data structure. The programming data type is the category that determines the data format to be used in the programs, such as arrays, structures, enumerator, and event pointers. In C, a user defined type or structure, is the most useful data format. It can form a variety of data structures when combined with pointers, such as link lists, queues and stacks. Furthermore, system provided data structure is the category of data types which are provided by the system. Here "system" refers to Sun C's compiler as well as the SunView Programming System. It includes some of the client data, Pixrect buffers (a kernel-based data storage system), and memory allocators. All these data types occupy the space of virtual memory and communicate to each other in one way or another.

5.3.1 "C" Data Types For Local Manipulations

Most of the data types can be generated by C's declaration of *structure, enumerator,* and *union.* The *structure* is a very useful data format declaration because it can be used to build a variety of data listings, such as link lists, queues and stacks. Each node or item on the list is a structure. Figure 5.4 is a practical example of link-list. It stores each image as a node of the whole list for search, insert, and delete. It can be designed to hold as much information as the programmer desires. Thus, a link-list is just like a file system, where each file has its own information header and of body. The files can be easily saved and extracted by searching throughout the list. These kinds of data structures are designed for local use (here "local" refers to the domain boundaried by the interfaces). *Enumerator* is look-up table to store sets of known data. *Union* is normally designed to allocate a part of memory to be shared by different types of the data.

The *Link List* structure has two types: *single-linkage list* and *dual-linkage list.* There is always a starting pointer marks towards the first node of the list. The difference between the two types is that the *single-link list* has only one pointer, which indicates either its last node or its next node, while the *dual-link list* has two pointers directing both to the addresses of its last and next nodes. Thus, the *dual-link list* is easier for searching and relocating the nodes, but the *single-link list* takes less memory and time for deleting and inserting. Figure 6-4 illustrates a practical implementation of the *dual-linkage list* for storing the images declared by C's structure.

A *Queue* is a "first-in first-out" list. It has two pointers. One pointer always indicates the bottom of the table, which is used for extracting the item. The other pointer notes the top of the queue where a new item is always added. In contrast, *Stack* is a "last-in first-out" table. It has only one pointer directing the top of the table, which is both the entrance and exit. Unlike the *Link List, Queue,* and *Stack* often have a fixed length, and usually do not allow inserting and deleting within the tables. A typical use of *Queue* in this package is to manage the position of each image displayed on the main canvas. The images can be display anywhere on the canvas and it can be overlaid above and even hidden behind other images. Each image can also be pulled to the front of or pushed behind other images. Therefore, designing a table to save and update each image's relative position on the canvas is the most efficient way to handle this. More detailed examples can be found from the source codes in Appendix I. For a complete detail regarding the contents of this subsection, please refer to *SunView Programmer's Guide* [20], *SunView System Programmer's Guide* [21] and *Pixrect Reference* [22].

```
typedef struct image {
        char *fname;
        int matrix;
        int image_type;
        Pixrect *pixrect;
        struct image *previous, *next;
        int x,y,w,h,zoom;
        Roi *roi_list;
        Roi *roi_selected
} Image;
```

Figure 5.4 A typical dual-linkage list, used for the images ever displayed on the main canvas before any "clear" and/or "delete" process is done.

5.3.2 SunView's Data Structure

SunView is an object-oriented programming package. It provides a whole range of pre-defined data structures for all kinds of its objects. It also provides a special type of data structure called *client data*, which allows some types of objects, such as frames, subwindows, and menus to carry some special application data.

The data structures of SunView objects are defined not only to ease the declaration of the data, but they are also defined as the carriers of the objects being transported from the program (software level) to the display (hardware level). Therefore, the programmer does not have to worry about the details of transferring the objects. The programmer simply uses them to declare variables as the other declarations do. Most of the internal information of each type of object data are preset as defaults or can be left blank.

One unique data structure, used by SunView's object-oriented programming to pass parameters across the function is called *attribute list*. By using *attribute list*, programmers can pass only needed parameters to the calling function (normally SunView's kernel functions). Thus, the programmer can create and modify objects by calling the corresponding procedures and set only those interested attributes.

Client data is another advanced feature provided exclusively by SunView. *Client data* allows the programmer to attach the user's own data to the objects declared. Thus, the programmer can easily tie closely related data together. The *client data* can hold any kind of data, either the regular C data types or SunView's objects data structures. One example of its application in this package is to put the image matrix and its corresponding information in the client data of the pop-up window. Therefore, there is no need to store those data as the global variable in order to pass them from function to function. Furthermore, the program is kept in a clean, professional style and easy to maintenance.

Next is an example source code from the shows some ideas of how the client data is used.

```
edge_map = (Boundary_Map*) malloc (sizeof (Boundary_Map));
window_set (pop_up_canvas, WIN_CLIENT_DATA, edge_map, 0);
window_set (pop_up_panel, WIN_CLIENT_DATA, edge_map, 0);
window_set (pop_up, WIN_CLIENT_DATA, edge_map, 0);
```

Here the attributes of the "edge_map" structure is stored as a client data of the pop-up window, and is retrieved in pop-up window's notifier function. This makes the "edge_map" easier to be obtained by other functions and SunView objects.

5.4 Remote Procedure Calls

Remote Procedure Calls (RPC) [18] are high-level communications paradigms which allow network applications to be developed by way of a specialized procedure calls which hide the details of the underlying networking mechanisms. It implements a logical client to the server communications system designed specifically for the support of network applications. With RPC, the client (normally a single application procedure or process) makes a procedure call, which sends requests to the server as necessary. When these requests arrive, the server calls a dispatch routine, performs whatever service is requested, sends back the reply, and the procedure call returns to the client. A simple example is making a call to `malloc()`, which asks the system for an item of memory.

The RPC is not only used to communicate between processes on different machines, but it also works for communication between different processes on the same machine. This is what has been implemented in building the Attenuation Correction Tool.

5.4.1 The RPC Model

The operating system normally carries two types of procedure call, *remote procedure call* and *local procedure call.* In the local case, the caller places arguments in a procedure in some well-specified location (such as a result register). It then transfers control to the procedure, but eventually gains that control back. At that point, the results of the procedure are extracted from the well-specified location, then the caller continues execution.

The *remote procedure call* (see Figure 5.5 on page 79) is similar to the *local procedure call* in which one thread of control logically winds through two processes ---- one is the caller's (or the client's) process, the other is the server's process. In other words, the caller process sends a call message to the server process and waits (blocks) for a reply message. The call message contains the procedure's parameters. The reply message contains the procedure's results. Once the reply message is received, the results of the procedure are extracted, and the execution requested by the caller is resumed. On the server's side, the process is dormant awaiting the arrival of a call message. When one arrives, the server process extracts the procedure's parameters, computes the results, sends a reply message, and then awaits the next call message. The advanced usage of the RPC protocol may ensure that the caller's process has the

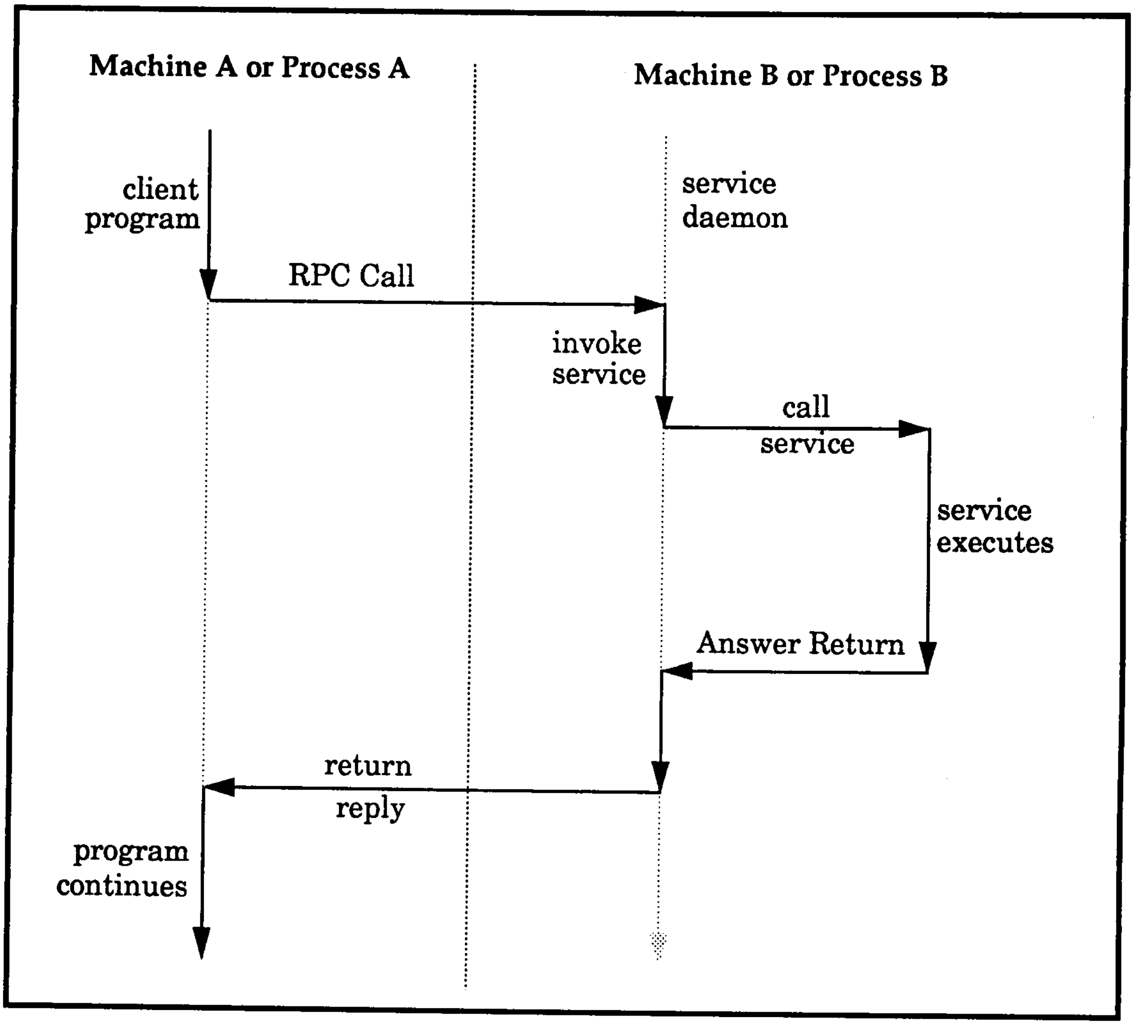

Figure 5.5 Remote Procedure Call Model

control while waiting for the reply message, and enables the server's process to block the incoming calls while working on the current caller's request.

5.4.2 Applications of RPC

In the application of the Attenuation Correction Tool, the program utilized "Colortool" and "Filer" provided by CTI, Inc. These two service processes communicate through the RPC. During implementation, these two tools were identified differently. "Colortool" was defined as a "mandatory" service tool, but "Filer" was noted as a "preferred" service tool.

"Colortool" provides variety of colormaps and interactive rescaling options, so that the gray-level image displayed on the screen can be mapped by different color maps to improve the visual resolution of the images. Whenever the user chooses a particular colormap from "Colortool", the colormap of the images is changed accordingly. "Colortool" is required every time the Attenuation Correction Tool is used because the canvases of the tool needs the colormap to display gray-level images. In practice, whenever the Attenuation Correction Tool takes control, it always checks whether the "Colortool" is active or not. If not, it will first run the "colortool". If the system cannot run "Colortool", for example in the situation that the window system is busy or the path to "Colortool" is not set properly, the process will exit. "Colortool" is always used whenever any image tool in CTI's PET System (CTI's Imagetool, Hearttool, Volumetool, as well as the Attenuation Correction Tool) is in use. Since "Colortool" only receives interaction from the user and the sends the colormap to its client tools, it is actually the controller of the colormap of all its clients. Whenever the user wants to change the colormap on the screen, the change must be made within "Colortool" window for the desired colormap, which is then sent to all the other windows with whom "Colortool" has client-server relationships. Then, those windows change their colormap accordingly. Therefore, "Colortool" acts like a master rather than a servant.

"Filer" is used for searching the image files throughout the disk(s). Unlike "Colortool" which is always required, "Filer" performs like an auxiliary service process. For example, in the attenuation correction tool, there is a "Filename" button on the main panel. Clicking it will engage "Filer" (calls the server). When the "Filer" window pops up, the user can choose the file by highlighting the filename in the list window (a simulated TTY subwindow) of "Filer". One can then go back to the tool's panel, and click the "Filename" button again (issues a request for a return message). "Filer" is iconified, but the highlighted selection of filename goes to the panel (the server returns the message and stands-by). If "Filer" is not available from the user's system, the user can simply type the filename onto the panel. Thus, "Filer" merely simplifies the procedure of searching for the wanted file and typing the filename on the panel.

CHAPTER 6. USER'S MANUAL

In this chapter, a detailed, step-by-step introduction of the Attenuation Correction Tool is given. The general procedures of attenuation correction via this package can be followed by the order given here. All the functions will be introduced even though not all of them will necessarily be used in all the cases.

- Getting Started
- Loading Transmission Images Files
- Displaying Images
- Enhancing Transmission Images
- Automatic Thresholding for Anatomic Segmentation
- Interactive Boundaries Redrawing
- Mapping Attenuation Correction Factor
- Line Integration for Attenuation Correction Sinogram

6.1 Getting Started

"Adaptive Attenuation Correction Tool" (see Figure 6.1 on page 83) was developed under the SunView environment. As long as the user is within the SunView Window System and the corresponding path is set, one can easily start up the tool from any terminal-simulated shell window by typing "atcrtool &". The addition of am-

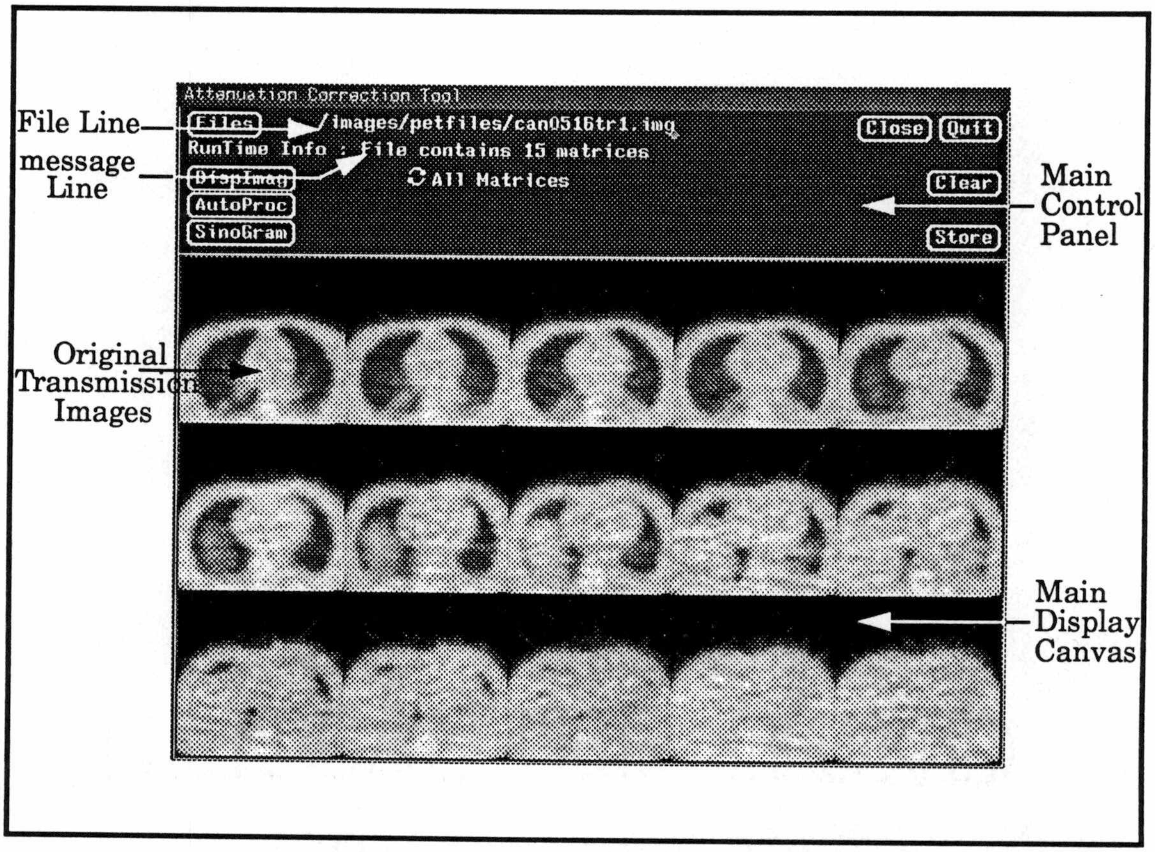

Figure 6.1 The Adaptive Attenuation Correction Tool (main window)

persand will make the tool run in the background. To be more efficient, this command can be built into the rootmenu so it can be driven through choosing the pull-right rootmenu on the console's background. For more information about this option, please refer to *SunOS User's Manual* [17].

The Adaptive Attenuation Correction Tool runs completely under its own window architecture as well as cooperating with some of the utility tools developed by CTI, such as "Colortool" and "Filer" (see Figure 6.2 on page 84), through RPC (Remote Process Communication). The Adaptive Attenuation Correction Tool itself contains two basic subwindows, the control panel and the display canvas. For further details about the software developed by CTI, refer to *Operating Instructions: Positron Emission Tomography System* [19].

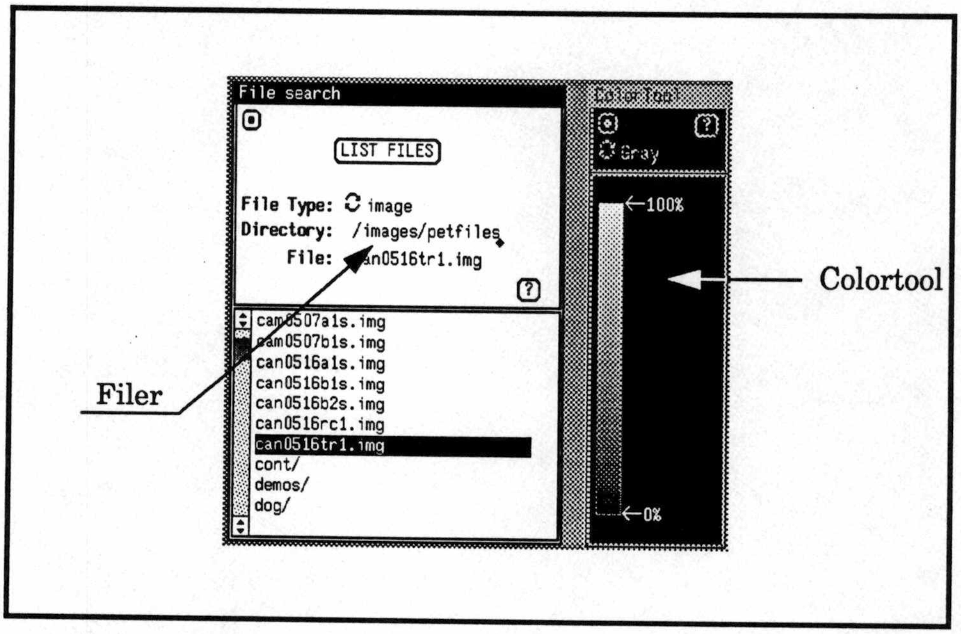

Figure 6.2 Filer and Colortool (Courtesy of CTI, Inc.)

Most of the basic commands to manipulate images (excluding those to segment images and detect boundaries, interactive graphic overlaying for boundaries adjustment and attenuation coefficients mapping, which are conducted through a separate pop-up subwindow) are issued through the control buttons on the main control panel and through the pull-right menus on the main display canvas (refer to the subsequent sections). The resulting images are then shown on the canvas while the run-time information is fed back onto the message line of the control panel. In the next six sections, the adaptive attenuation correction tool will be introduced using a step by step illustration.

6.2 Loading Transmission Images

Before any processing, transmission images must first be loaded into the tool. There are two ways to load a transmission image file. The user can simply type the name and path of the desired image file on the file line after the "filename" button. The other option is that the user can click the "filename" button to engage the "Filer", and then choose the image file one wants within the "Filer" tool. Next, the user clicks the "filename" button on the main panel again. The path and name of the chosen image file will automatically appear on the file line right after the "file" button (see Figure 6.1 on page 83).

The user must be aware that the attenuation correction tool accepts only the transmission image files with extension name "*.img" (CTI's definition). Should another type of image be loaded, an error message will be posted onto the panel's message line right after "RunTime Info" label.

6.3 Displaying Images

There are three types of images that can be displayed on the canvas: PET transmission images, enhanced transmission images, and attenuation coefficients maps. The last two image types are generated during the process and their details will be introduced in Section 6.4 and Section 6.6, respectively. By clicking the "DispImag" button on the control panel with the default mode setting, the chosen transmission image file will be loaded into system memory from the disk and then displayed on the canvas. The rest of this section examines image types, display modes, and position handling menus.

6.3.1 Types of images to be displayed

By default, the display button "DispImag" is always set to display the original transmission scans, the other two types of images can be displayed through the button's pull-right menu and the existing images can then be displayed in either mode mentioned in the next part. If the image does not exist for any reason, an error message will appear on the panel's message line (see Figure 6.3 on page 87).

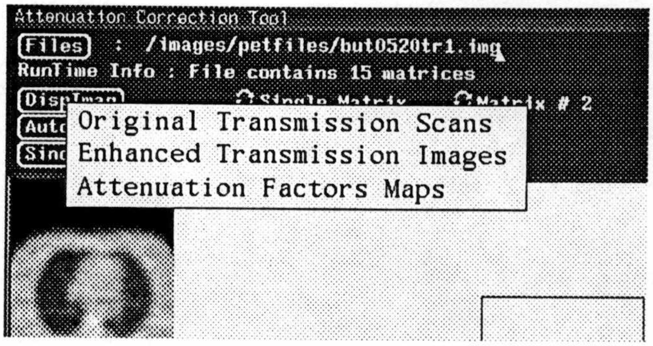

Figure 6.3 Display Button's Pull-Right Menu With Display Options

Enhanced transmission images are generated after image enhancement, which will be discussed in Section 6.4. Attenuation coefficients maps are generated after the procedure is finished.

6.3.2 Image displaying modes

There are two modes of displaying which can be chosen, either the whole set or an individual image. A set of transmission images normally contains 15 or 31 slices of images. Thus, this option enables the user the flexibility of checking images and accessing the specified image. These modes can be set from the cycles to the right of the Display button "DispImag" (see Figure 6.4 on page 88).

While displaying whole set of images, the images are displayed successively in order from left to right, then from top to bottom. At the bottom-right, the process returns to the top-left again. The process is based on the availability of the display canvas's height and width. After resetting (by pushing the "clear" button), the first displaying position of displaying is always in the order from top-left corner of the canvas.

For displaying a single image, the image position can be chosen through a pull-right menu on the canvas. Selecting this option causes a red box to appear on the canvas. Move the red box around to the desired position for next image (see Figure 6.4 on page 88). A complete explanation of positioning the image will be given in the next subsection.

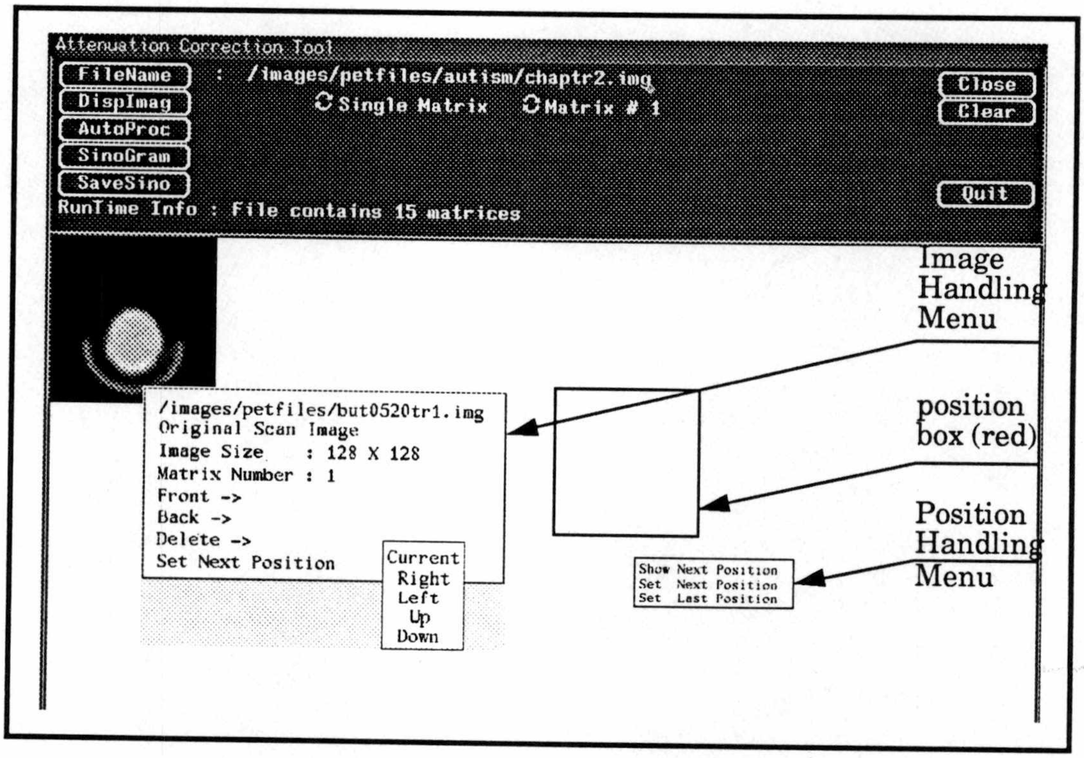

Figure 6.4 Image Display Handling Menus

6.3.3 Display handling menu

There are two types of pull-right menus on the display canvas, the *Image Handling Menu* and the *Position Handling Menu* (see Figure 6.4 on page 88). Normally, these menus contain options designed for the single image display mode as well as information regarding the chosen image. If a whole set of images are displayed according to the option(s) chosen from the canvas pull-right menus, the menu choice will affect only the first image of the set.

When the cursor is on the background of the canvas (see Figure 6.4 on page 88), the pull-right menu is engaged by the mouse's right button from the *Position Handling Menu*. The *Position Handling Menu* contains three parts: show next position, set next position and set last position.

<u>Show Next Position</u> displays the next available image displaying position. Normally, the next available position is the next logical image position. A red box will appear for that position (the same order as mentioned in paragraph 2, Section 6.3.2).

<u>Set Next Position</u> sets the position for displaying the next image. When this option is engaged, a red box will appear on canvas. The user should move the box around the canvas by moving the cursor to choose the preferred position. Then, the user should push down the left mouse button, the red box will remain and the next image will be displayed in the red box.

<u>Set Last Position</u> will allow the next image to be displayed over the last image displayed.

The *Image Handling Menu* is engaged if the cursor is pointing to a specified image. This menu gives users not only the option to relocate image, but information about the specified image itself (see Figure 6.4 on page 88).

The information portion of the menu occupies the first four lines in the menu. The first line tells the file name and path to which the referred image or the original image belongs. The second line shows the type of image. The third line gives the image size. The fourth line indicates the matrix number of original image.

The option portion contains four or five lines, depending upon what type of image is selected. The first three lines provide an option to display the preferred image, especially when several images are overlaying each other. Front brings the image to the front. Back pushes the image behind other images. Delete removes or erases the image. Set Next Position has its own pull-right menu which gives the option of positioning the next image around or even above the current one. If the active image is an enhanced transmission image, there is one more option called Pop-Up Window. This option creates the pop-up window for further operations (clicking the left button while pointing to this type of image activates the same function).

6.4 Image Enhancement

All the procedures mentioned above relate to input and display of the images. The procedures to be introduced now will lead to the final goal of this tool, attenuation correction. Therefore, the following procedures are not available if the entire set of transmission images has not been displayed on the canvas.

Usually, the original transmission images are poor because of limited resolution of the PET scanner. Thus, enhancement is extremely important for further segmentation and attenuation correction factors mapping.

The operation of image enhancement includes most of the procedures which were discussed in Chapter 3. These procedures are *image smoothing*, *image enhancement filtering* and *intensity modification*. To enhance a transmission image (or the whole set of images), click the "ImagProc" button, adjust the options on the panel (see Figure 6.5).

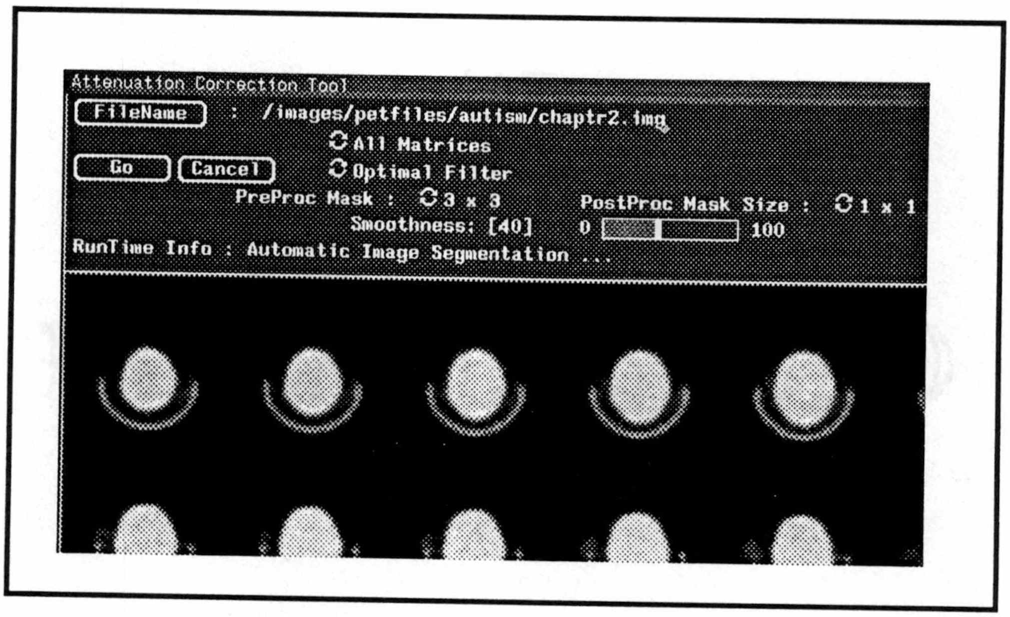

Figure 6.5 Image Enhancement Panel

The AACT provides default parameters for all four options, *filter type*, *PreProc mask size*, *PostProc mask size* and *smoothness*. However, the user can freely adjust any of them to fit the situation of individual image. There are two types of optional enhancement filters. “Optimal filter” is the actually the modified inverse filter, “high pass” filter is the “windowed” filter (see Section 3.3 for more details). The “PreProc Mask” is to set the mask size of both median filter and low-pass filter for image smoothing (see Section 3.2). “PostProc Mask” is to set the mask size for local intensity correction (see Section 3.4.3), while “smoothness” factor is actually the weight value of Equation 3.18 for global intensity modification (see Section 3.4.2).

As with displaying, the user can choose to process the whole set of images at once by choosing “All Matrices”, or process any preferred single image by either choosing “Single Matrix” and “Matrix #” or directly clicking on the middle button of the mouse on the desired image on the canvas. The second option always displays the enhanced image over its original version.

The user then click on “GO!” to engage the procedure of image enhancement, or hit “Cancel” to quit.

During the process, a set of moving “>”s and “<“s can be seen on the “message line” which indicates the forward FFT and inverse FFT respectively for frequency filtering. After an image has been processed, the enhanced version of the image will be overlaid on the original transmission image.

6.5 Edge Detection For Anatomic Segmentation

The segmentation process actually contains two parts, automatic thresholding for boundary detection, and interactive boundary repairing. This section will introduce the automatic edge detection for anatomic segmentation, based on the difference of the transmission scan intensities of each kind of tissue. The detail algorithm of automatic segmentation can be found in Section 3.5. Interactive edge repairing provides the user with the capability to correct errors which occurred during automatic segmentation.

Automatic segmentation and interactive edge repairing are two separate parts. They can be performed either consecutively or independently. This means that if the result of automatic boundary detection is adequate, the second part, which is interactive adjustment, can be skipped. If the result from automatic boundary detection is incorrect, the user can interactively redraw the boundary onto the image, or simply correct the boundary.

The operations mentioned here are conducted under a separate pop-up window, which is the platform for both Image Segmentation and Attenuation Correction Factors Mapping (see Figure 6.6). The pop-up subwindow provides the platform for not only segmentation (both automatic thresholding and interactive repairing), but it also provides for attenuation coefficients mapping which will be discussed in Section 6.7. The pop-up window is also a single image based processing window. To process the desired image slice, the image must have been enhanced as discussed in previous section (see Section 6.4). Moving the cursor onto the desired image (either original or enhanced), and pushing the middle mouse button causes it to appear. This window zooms the original image three times the image's initial size and includes the detected edges along with the background image (see Figure 6.6).

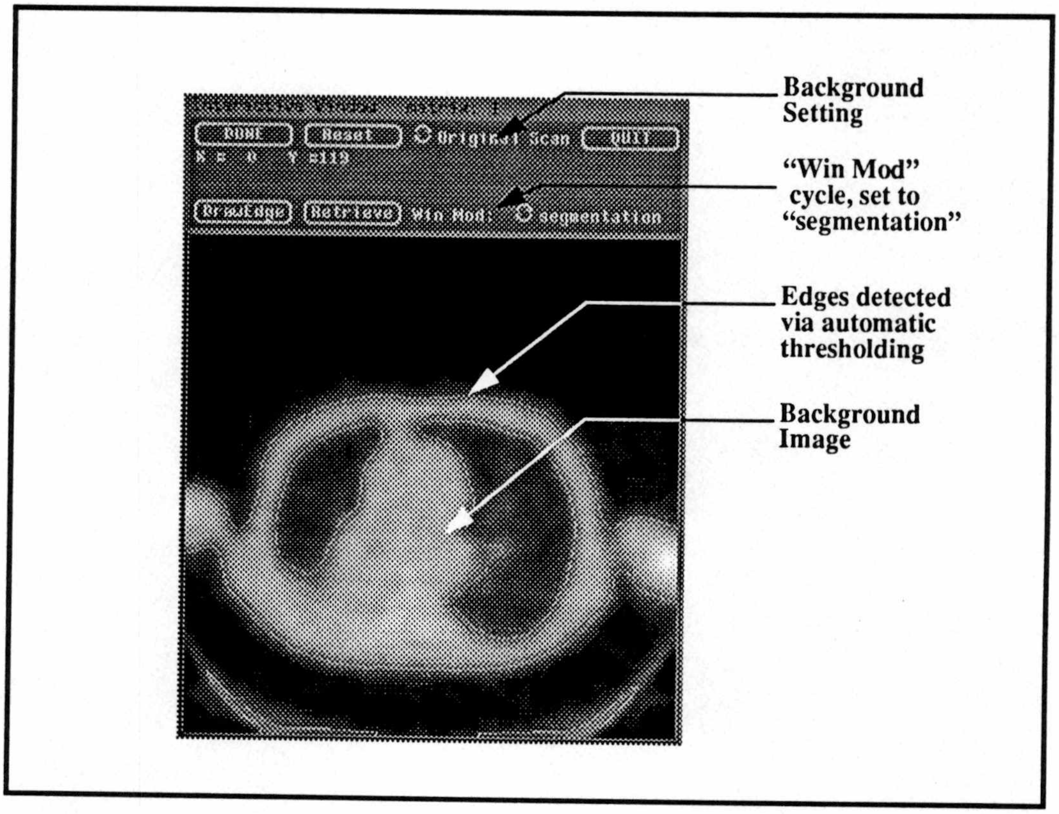

Figure 6.6 Pop-Up Window for Image Segmentation and Attenuation Factor Mapping

To engage the automatic image segmentation, click the "DrawEdge" button on the subwindow's panel. A pop-up panel (see Figure 6.7 on page 95) will appear which starts the automatic segmentation process.

The pop-up panel provides two options enabling the user to achieve optimal edge detection. The "Threshold Mode" provides different levels of threshold from 1 to 4 as well as "auto". Level 1 to level 4 represents increasing thresholds while the "auto" mode combines levels 1, 2 and 3. "Noise Removal Level" measures the length of the open, isolated, and small pieces of boundaries. The user can change the value easily by moving the slider. For more details about the thresholds and noise removing, the user can see Chapter 4. When "GO" is pressed, threshold is then engaged and the resulting boundaries will be overlaid upon the image.

The user can choose several different modes of thresholding, or simply choose "auto" to automatic step through modes 1, 2, and 3. The background image can be switched among "original scan", "segmented Img", and "blank" for better visual sensitivity.

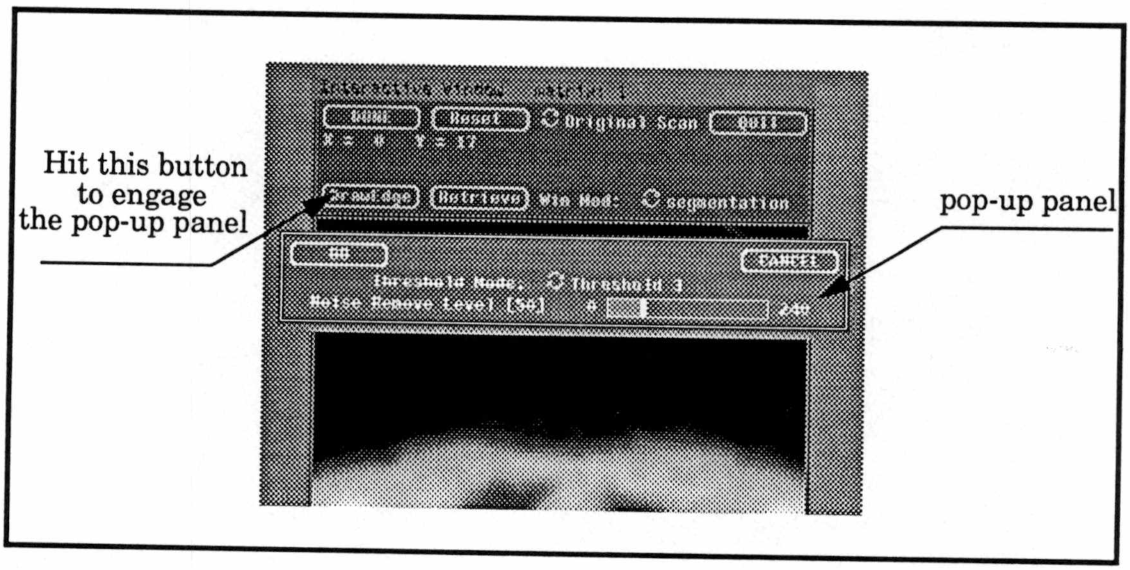

Figure 6.7 Pop-Up Panel for Automatic Segmentation

Normally, the output of automatic boundary detection will not be very smooth. This process often yields some zig-zag edges along with some false contours due to the image noise. Thus, further interactive adjustment of these edge pieces is necessary.

6.6 Interactive Boundary Repairing

Interactive boundary adjustment was designed for two purposes --- direct drawing of the boundaries and amendment of the created boundaries. All the options in this part are completely "menu driven" through the pull right menus on the sub-window's canvas. In this option, the "Win Mod" on the panel must be set to "segmentation" (the default setting) to invoke the interactive boundary adjustment mode.

During interactive repairing of the edge and later attenuation factor mapping, the left, middle and right mouse buttons each has its own function. According to convention, the left button is the "select" button, the middle button is the "execute" and "confirm" button, while the right button is the "cancel" and "menu" button. A typical menu-driven operation follows the procedure: (1) choose the option from the menu using the right button on the mouse, (2) select the object to be operated with the left button on the mouse, and (3) execute the operation by clicking middle button on the mouse or cancel the operation by pushing the right button on the mouse.

The pull-right menu set in this option contains two separate parts: the *General Processing Menu* and the *Single Edge Handling Menu*. Both of these are activated by pushing down the mouse's right button when no edge is selected.

6.6.1 General processing menu

The *General Processing Menu* provides several manipulation functions to apply on the entire set of the boundaries (see Figure 6.8 on page 98). This menu is operational when no specified edge is selected (the boundaries are green) and has three functions:

1. Undo any manipulation done by this menu set (both General Purpose Menu and Piecewise Handling Menu),
2. Redefine the mutual relation of the edges detected through automatic thresholding,
3. Draw new edges, clear tiny segments of edges and even delete the entire image edge map.

6.6.2 Single edge handling menu

The Piecewise Handling Menu appears only if a piece of boundary is selected by the cursor. To activate it, move the cursor onto the edge of interest. The edge is hit if the cursor switches into a red bullseye (called "Hit Edge Cursor"). Next, click the mouse's left or middle button to change the selected edge from green (unselected status) into red (selected status). The "Single edge Handling Menu" can then be brought up through the canvas' pull-right menu (see Figure 6.9 on page 98).

The Single edge handling Menu contains two major parts: changing the shape of the selected boundary and cutting or removing part of or even the entire selected edge. The first part has three options and the second part has four options.

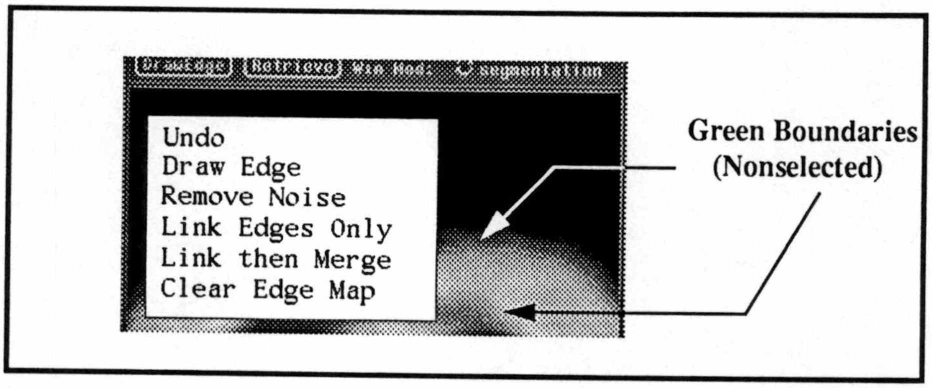

Figure 6.8 General Purpose Menu On Interactive Window Canvas

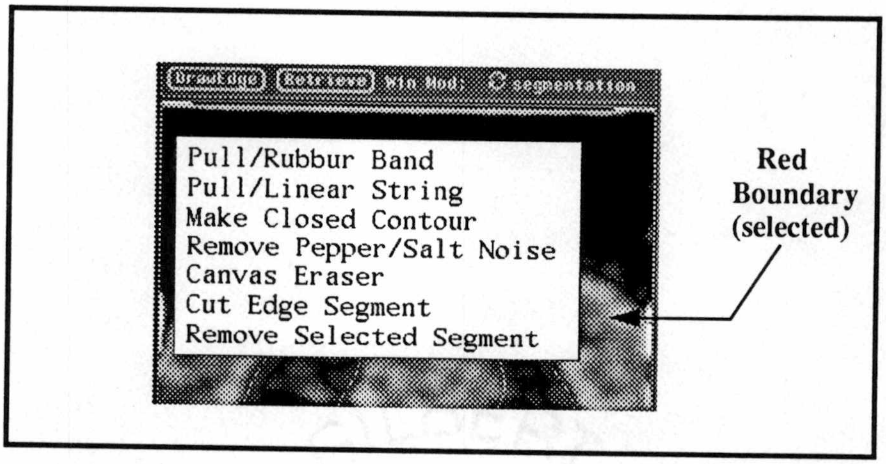

Figure 6.9 Piecewise Handling Menu

6.6.2.1 Changing the shape of selected boundary

There are two kinds of operation to change the shape of a selected boundary, "pull" and "close". "Pull" changes the contour of part of the boundary. "Close" completes an open contour.

There are two kinds of "pull" operations: rubber-band and line-string. The major purpose of "pull" is to change the local shape of the boundary without interfering with the remote part of the edge. As mentioned at the beginning of this section, one can select the part of edge using the left mouse button, move the mouse around to pull the selected piece of edge. First, one must confirm the position by clicking on the middle button, or cancel this option by hitting the right button. When selected and pulled, the color of selected yet unconfirmed part of the edge is yellow. When confirmed, the edge will turn green and the canvas menu status will go back to the General Processing Menu. Should the user cancel the operation, the edge segment will return to the original shape, and the color will remain red indicating the canvas status is unchanged.

The second operation is "close". To use this option, the edge must first be chosen via the left mouse button. Next, the user can simply choose the option from menu and click on the left button to select. The selected edge will turn from red to yellow. Next, the user can click on the middle button to execute and confirm. A straight line will directly link the two ends of the opened contour of the edge and close it. The closed edge will then turn green, and the canvas status goes back to the General Processing Menu. The user can also click on the mouse's right button to cancel and keep the canvas status in the Single Edge Handling Menu.

6.6.2.2 Cutting and/or removing the edge segment

In this part, four different operations can be chosen; each might be able to destroy partly or wholly the selected edge. They are: (1) Remove Pepper and Salt Noise, (2) Cut Edge Segment, (3) Canvas Eraser, and (4) Remove Selected Segment.

"Pepper and Salt Noise" refers to the tiny segments of boundaries which are left through other operations. The user will find that the same option appears on the General Processing Menu and is actually for the same purpose.

"Cut Edge Segment" is the reverse operation of the "close" function mentioned in Section 6.6.2.1. It clips the piece chosen, and removes it so that the remainder of the boundary is left open.

"Canvas Eraser" is a free-erasing operation When this option is chosen from the menu and the left mouse button is pushed down, the "Eraser Cursor", a red solid rectangle with a transparent "E", will replace the original cursor. Moving the "Eraser Cursor" around while pushing down the left mouse button causes the pieces of the selected edge (red) which are covered under the "Eraser Cursor" to turn yellow. Clicking the middle button will leave only the untouched part of edge in green and the canvas menu status goes back to the General Processing Menu. If the right mouse button is pushed, the selected yellow pieces will go back to red and this operation is canceled.

The “Remove Selected Segment” operation is actually to remove the whole selected edge. After choosing the option from the menu and clicking on the left mouse button anywhere on the canvas, the selected edge will turn yellow. To confirm, click the middle button to remove the whole piece of edge, or cancel it by clicking on the right button.

Normally, the interactive package is to assist segmentation. The user is expected to choose the optimal filter and smoothness for reducing the processing time on the interactive package.

6.7 Attenuation Factor Map

Since all the anatomical regions are well segmented after the above procedures, the user now can assign each region with their corresponding attenuation factors, a process called “Attenuation Coefficients Mapping”.

The use of the attenuation coefficient map and how to perform the processing are included in this section. Users are advised to switch the color table to “Rainbow” using Colortool (see Figure 6.2 on page 84), so the user can distinguish the value of an attenuation coefficient by its color on the canvas (see Figure 6.10).

Before engaging this mode, the user must make sure that all of the unnecessary edge pieces are removed. The user must also make sure that each of the remainder edge pieces is anatomically meaningful, and be sure each segment’s boundary is closed. Next, the user should switch the “Win Mod” cycle from “segmentation” to

"ACF defining". This switch will automatically change the canvas pull-right menu. The new menu is exclusively used for attenuation factor mapping and called "Attenuation Factors Menu" (Figure 6.10). There are five preset attenuation coefficient values for bone, soft tissue, patient bed, lung, and air. Each factor is represented by a preset color on the pop-up canvas, and the actual value is saved separately in an internal attenuation map.

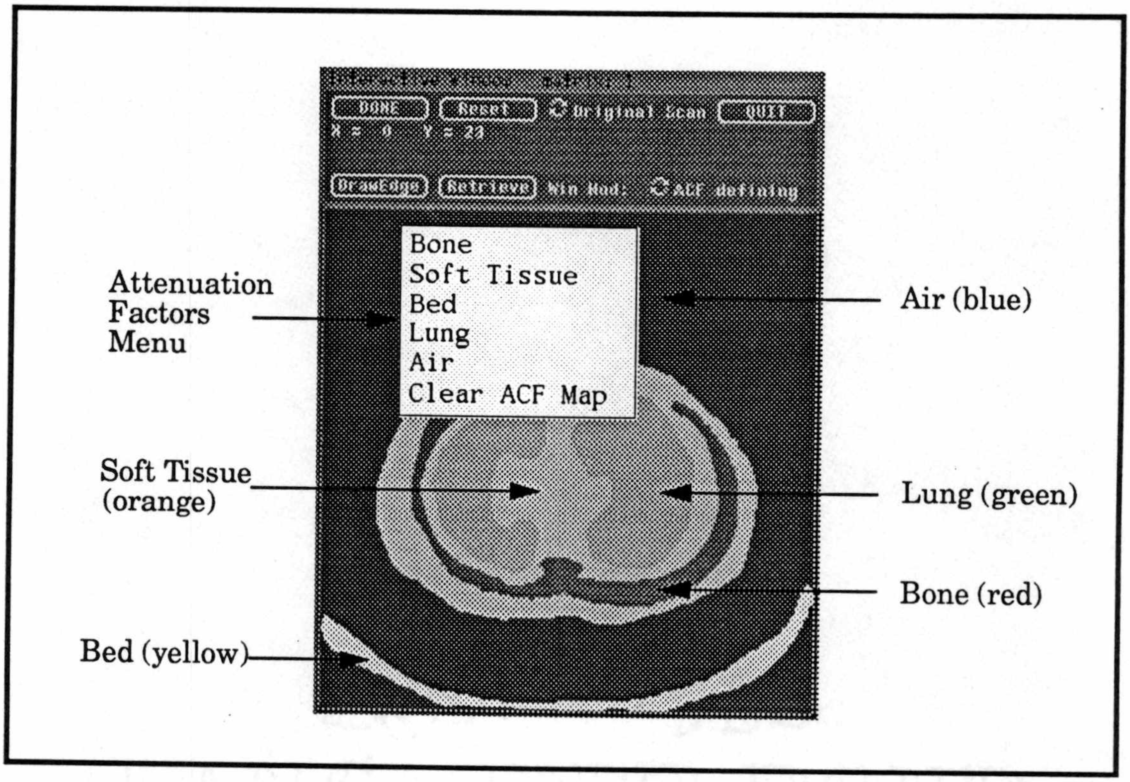

Figure 6.10 Attenuation Factor Map with Attenuation Factor Menu

To fill the regions with selected attenuation factors, simply choose the factor from the "Attenuation Coefficient List" menu through the right mouse button, move the pointer into the region desired and click on the left mouse button. The region within the closed boundary is filled by a preset color, and the selected value is written into a separate internal map in system memory. Once a region is processed, the left button mode is locked to the chosen factor. The user can repeat the above processing for other regions if they are supposed to be assigned with same factor. To choose another factor, click on either the middle or the right mouse button. The left button mode will be unlocked, and the user can choose another factor through the "Attenuation Coefficients List" menu. After all the desired regions are assigned with appropriate attenuation factors the user must press the "DONE" button on pop-up window's panel to put the attenuation factor map back onto the main canvas (and the size is also zoomed down to its original size, normally 128 by 128). The user can then process each image until the last one is finished. At this time, total processing time for an uncomplicated transmission image scan is approximately 15 to 30 minutes.

6.8 Generating Attenuation Correction Sinogram

After the entire set of transmission images is segmented and mapped with attenuation correction factors, it is time for the last step in this tool: calculate the line integral and exponential to create the attenuation correction sinogram.

The user should click on the "SinoGram" button on the main panel, the attenuation correction tool will automatically compute the line integral and exponential of summation of each slices. The line integral is calculated on each image from 256 projection angles distributed evenly throughout the semi-circle; each projection has 192 beams. For the attenuation correction sinogram, the summation of each beam projection is modified by an exponential. The data is saved on disk with the "matrix" attenuation file header as defined by Siemens/CTI PET System [26]. The computing time of forward projection takes about 20 seconds per slice on a Sun Sparc2 workstation.

After finishing the computing, the user must save the sinogram into a disk file. Click on the button "SaveSino", a small window will pop up, with a default file name on it (the file type must be attenuation file (Siemens/CTI's definition) with the extension name ".atn"). The user can change the file name as desired or leave it unchanged. After specifying the output filename, the user must click on the "GO" button to process the calculation and save. This process is conducted successively from the first image of the entire set to the last one. After the whole process is finished, the main panel is reset, and the user can clear the canvas to process the next set of transmission images.

CHAPTER 7. SUMMARY

7.1 Conclusions of this project

The purpose of this research was to reduce the transmission scan time while still maintaining good quantitative PET studies. The approach is to combine the interactive segmentation and image processing to achieve the best possible results at the lowest possible consumption of both patient's in-bed time and operating time. The design work has focused on reducing noise and distortion in the transmission scan image, thus providing more accurate attenuation correction sinogram.

7.1.1 Image processing approach

The image processing approach is based on the image degradation model study. It is made up of several consecutive parts: image smoothing, enhancement, correction, segmentation, and edge detection.

The degradation model is based on a comparison of a normal transmission image versus a less-than-ideal transmission image with the same internal attenuation structures. When "less-than-ideal" is mentioned here, the term means that there is no way to get a perfect image for comparison. Here, the "less-than-ideal" transmission is acquired through a longer transmission scan because longer scanning time generally yields better image quality with lower statistical noise and distortion.

Image smoothing as the first step is essential since it attempts to make the system distortion approximately linear. The procedure includes both median filter and low-pass filter to clean up the random noise and increase uniformity.

Image enhancement uses a modified inverse filter to enhance the structure of interest by emphasizing a few frequency bands where there is known structural information. The filtering method is further incorporated with intensity modification to correct the intensity distribution which was altered after filtering.

Image segmentation and edge finding is the final step of image processing in the Attenuation Correction Tool. This procedure locates the boundaries of structures of interest and removes some of the remaining noise segments.

At this point, the images are almost ready for attenuation factor filling and sinogram computation. If the operator is still not satisfied by the results of the above processes, he can select the interactive package to redraw the edges which are incorrect.

7.1.2 Interactive Drawing Package

The interactive drawing package allows the operator the option of either directly drawing the edges on top of the image or changing the existing image boundaries. In addition, assigning attenuation coefficients must be done manually using the interactive package.

In drawing, the operator is able to use the mouse and cursor on the screen to draw, remove, relocate, and change the shape of the edge segment selected, and even make an opened edge segment closed.

In assigning attenuation coefficients, there are several fixed-value attenuation factors which the operator can simply click-and-paint. The filled image is then called the attenuation coefficient map, and is ready for immediate attenuation correction factor sinogram calculation.

7.1.3 Overall performance

The primary purpose of the Adaptive Attenuation Correction Tool is to reduce the total scanning time of each patient. Normally, a conventional transmission scan for attenuation correction requires an additional 20 minutes of bed time per emission scan. Experiments shows that using this tool, the transmission scan for each emission scan can be reduced to 5 - 10 minutes while still getting comparable quality of emission data (Chapter 4). This can potentially save between 1 and 2 hours of bed time in a clinical center treating 6 - 10 patients each day. Thus, there are savings in terms of both patient comfort and increased throughput. Meanwhile, in case of the worst situation (see Section 4.3), when an emission study lacks transmission image for correction, the operator can use AACT to process the attenuation correction based on the uncorrected emission image, and this procedure takes only 30 minutes.

The tool is designed for fast and easy use. Operators who are familiar with Sun Window system and PET software (from Siemens/CTI) will find themselves getting used to it quickly. Each operation is designed to be user-friendly and confirm to

SunView standards. Most of the procedure in this tool also provide immediate feedback. Processing speed is faster if used on Sun SparcStations, and the results from automatic segmentation are generally good. Thus, operator interaction is minimized. Furthermore, attenuation correction is no longer a black box which is blind to the operator. This means operators have more access to quality control throughout the whole process, and can generate better quantitative PET results (see Chapter 4 for more details about the system evaluation).

7.2 Future Work

There are several potential improvements in the current work and areas of additional work that can be performed. Both are addressed below.

7.2.1 Second Thought On Current Work

This project addresses only one of several methods which may be used to process the transmission images. In cases of poor quality images, the image processing in this tool is less accurate and the user's interaction is tedious. Thus, faster computing algorithms should be used. The routines for interactive drawing need to be polished since there is still some programming overhead remaining in the package. In its present form, this tool requires a minimum of a Sun Sparc 2 in order to be efficient in processing.

Transmission scan through different parts of the body need different types of image processing procedures. Automated protocol should be established for different types of transmission images.

The Adaptive Attenuation Correction Tool functions in the SunView window system, Sun's own unique window system. The advantage of this window system is that it is kernel-based window system. Therefore, processing data, displaying and refreshing the windows are fast. Second, Siemens/CTI has all the PET processing software utilizing SunView. Thus, it is good for keeping consistency in PET image processing. The disadvantage is that it is not compatible with the X window system. The X11 window system is fast becoming the industrial standard. Because the X window is a server-client window system, machine and operating system independent, it is virtually portable around all kind of machines, from PC to Cray. Furthermore, X window is network transparent and the window can be passed through the network system. Either from the point of convenience or portability, conversion into X window system would be useful.

7.2.2 Recommendation For Further Research

Further research can shift the focus from the visible transmission image to the invisible sinogram. This would save time in reconstructing transmission images and possibly yield better accuracy since there would be no reconstruction artifacts. Such a process would be completely automatic and require no interactive work for the operator.

Focus could also be shifted to non-transmission scan attenuation correction. Some agents in PET, like ACBC, even in the raw image, reveal some of the attenuation structural information. Here, complete interactive drawing by the operator may be necessary. These two approaches may be done together, since the sinogram approach can be complimentary to the emission concept.

LIST OF REFERENCES

[1] Hoffman EJ, Phelps ME, *Positron Emission Tomography: Principles and Quantitation*, New York, New York: Raven Press; 1986.

[2] Huang SC, Hoffman EJ, Phelps ME, Kuhl DE: Quantitation in Positron Emission Computed Tomography: 2. Effect of inaccurate attenuation correction. *J Comput Assist Tomogr* 3:804-814, 1979.

[3] Sorenson JA, Phelps ME: *Physics in Nuclear Medicine*, 2nd edition. Orlando, Florida: Grune & Stratton; 1987.

[4] Huang SC, Carson RE, Phelps ME, Hoffman EJ, Schelbert HR, Kuhl DE: A boundary method for attenuation correction in positron computed tomography, *J Nucl Med* 22:627-637, 1981.

[5] Bergström M, Litton J, Eriksson L, Bohm C, Blomqvist G: Determination of object contour from projections for attenuation correction in cranial positron emission tomography. *J Comput Assist Tomogr* 6(2):365-372, 1982.

[6] Ganti G, Ranganath MV, Mullani NA, Gould KL: A multi-resolution method for attenuation correction in positron emission tomography. *J Nucl Med* 30:880, 1989.

[7] Xu EZ, Mullani NA, Gould KL, Anderson WL: A segmented attenuation correction for PET. *J Nucl Med* 32:161-165, 1991.

[8] McCullough EC: Photon attenuation in computed tomography. *Medical Physics* 2(6):307-320, 1975.

[9] Gonzalez RC, Wintz P: *Digital Image Processing*, 2nd edition. Reading, Massachusetts, Addison-Wesley; 1987.

[10] Hoffman EJ, Huang SC, Phelps ME, Kuhl DE: Quantitation in Positron Emission Computed Tomography: 4. Effect of accidental coincidences. *J Comput Assist Tomogr* 5:391-400, 1981.

[11] Gullberg GT, Huesman RH: Emission and transmission noise propagation in positron emission computed tomography. Presented at the Society of Nuclear Medicine 26th Annual Meeting, Atlanta GA, June 26-29, 1979.

[12] Hoffman EJ, Huang SC, Plummer D, Phelps ME: Quantitation in Positron Emission Computed Tomography: 6. Effect of non-uniform resolution. *J Comput Assist Tomogr* 6:987-999, 1982.

[13] Castleman, KR: *Digital Image Processing*. Englewood Cliffs, New Jersey, Prentice-Hall; 1979.

[14] Otsu N: A threshold selection method from gray-level histograms. *IEEE Trans. Syst., Man., Cybern.*, vol.SMC-9(1):62-66, 1979.

[15] Marr D, Hildreth E: Theory of edge detection. *Proc. Royal Soc. London,* 207:187-217, 1980.

[16] Torre V, Poggio TA: On edge detection. *IEEE Trans. Pattern Anal. Machine Intell.*, PAMI-8:147-163, 1986.

[17] *SunOS User's Manual.* Sun Microsystems, Inc. Mountain View, California, 1990.

[18] *Network Programming Guide.* Sun Microsystem, Inc. Mountain View, California, 1990.

[19] Operating Instructions: *Positron Emission Tomography Systems.* Siemens/CTI, Knoxville, Tennessee, 1989

[20] *SunView Programmer's Guide.* Sun Microsystems, Inc. Mountain View, California, 1990.

[21] *SunView System Programmer's Guide & Pixrect Reference.* Sun Microsystems, Inc. Mountain View, California, 1990.

[22] *SunView System Programmer's Guide & Pixrect Reference.* Sun Microsystems, Inc. Mountain View, California, 1990.

VITA

Ming Xu was born in Shanghai, the People's Republic of China on March 25, 1965. He was graduated from Fuxin High School in Shanghai in July, 1983. In September, 1983, he enrolled in Shanghai Jiao Tong (National Chiao Tung) University, where he received a Bachelor of Science in Biomedical Engineering in July 1988. In 1985, he also received a one year medical fellowship in Shanghai Medical University.

He received a research assistantship from the Nuclear Medicine Department of the University of Tennessee Medical Center at Knoxville in January 1989. Since September 1989, he began the study of Medical Image Processing in the Department of Electrical & Computer Engineering of the University of Tennessee toward a Master of Science degree.